

THE UNIVERSITY OF MANITOBA

A METHOD FOR PERFORMANCE EVALUATION OF  
IMAGE INTENSIFIER FLUOROSCOPIC SYSTEMS

by

MARTIN YAFFE

A THESIS

SUBMITTED TO THE FACULTY OF GRADUATE STUDIES  
IN PARTIAL FULFILMENT OF THE REQUIREMENTS FOR THE DEGREE  
OF MASTER OF SCIENCE

DEPARTMENT OF PHYSICS

OCTOBER, 1973

WINNIPEG, MANITOBA



#### ACKNOWLEDGMENTS

I wish to thank Dr. A. F. Holloway and Dr. D. V. Cormack for their advice and encouragement during this project, and Dr. K. Hoshino of the Department of Anatomy who was kind enough to assist me with the microdensitometry. Mr. R. Walton and Mr. B. Pieper of the Department of Radiology, Health Sciences Centre donated many hours of their time in helping with the experimental work.

A special thanks is extended to Mr. Allan M. Wright for his valuable suggestions and computing assistance. The efforts of Mr. Art. Matrick who produced the diagrams and graphs and Ms. Phyllis Yaffe who typed the first draft are very much appreciated.

Finally, I would like to extend my thanks to the Manitoba Cancer Treatment and Research Foundation and its staff, which provided financial assistance and an excellent environment for carrying out this research.

A METHOD FOR PERFORMANCE EVALUATION OF  
IMAGE INTENSIFIER FLUOROSCOPIC SYSTEMS

MARTIN YAFFE

ABSTRACT

The need for an objective method for assessing the performance of image intensifier television fluoroscopic systems used in diagnostic radiology is discussed. Use of the Modulation Transfer Function (MTF) to quantify certain aspects of image quality is described. Sinusoidal response of an imaging system is determined by Fourier analysis of the square-wave response of the system.

Records of image quality are recorded on photographic and radiographic films and information extracted by scanning them with a Zeiss<sup>05</sup> microscope photometer used as a microdensitometer. Fourier analysis is performed on a digital computer using a Fast Fourier Transform algorithm.

A Delcalix light amplifier fluoroscopic unit part of a Picker Therapy Simulator system, was examined using these techniques. MTF measurements were made at the input phosphor of the intensifier and for the overall system. The system MTF was found to have fallen to 5% at a spatial frequency of .76 line-pairs per millimeter.

A video "line-selection" device was designed and built to permit more rapid MTF measurements from the composite video signal. Comparison of the overall MTF with that obtained from the video signal yields information about the contrast enhancement of the television monitor. It was found that this contrast enhancement was considerable and affected image detail perception to a large extent.

Table of Contents

I	INTRODUCTION . . . . .	1
	Limitations of Conventional Fluoroscopy . . . . .	1
	Need for an increase in image brightness . . . . .	2
	The image amplifier . . . . .	2
	Present state of fluoroscopy . . . . .	3
	Need for image evaluation . . . . .	4
II	METHODS OF IMAGE EVALUATION . . . . .	7
	Subjective methods . . . . .	7
	Objective testing methods . . . . .	8
	(i) Line spread function . . . . .	8
	(ii) Modulation transfer function . . . . .	9
	Practical measurement of MTF . . . . .	15
	(i) Fourier analysis . . . . .	15
	(ii) Application of Fourier theory . . . . .	17
III	EXPERIMENTAL METHOD . . . . .	20
	The square wave test pattern . . . . .	20
	Input to the imaging system . . . . .	21
	Microdensitometry . . . . .	24
	Characteristic curve . . . . .	29
	Calculation of MTF . . . . .	29
	Measurements on the imaging system . . . . .	31
	Output of the imaging system . . . . .	33

III (cont'd.)	
Output of the television camera . . . . .	35
Analysis of composite video signal . . . . .	39
IV ASSESSMENT OF THE EXPERIMENTAL METHOD	
MTF of primary imaging process . . . . .	43
MTF measured at the television monitor . . . . .	43
Influence of the television monitor -- contrast enhancement . . . . .	45
Raster lines . . . . .	47
MTF of the composite video signal . . . . .	47
Conclusion . . . . .	49
APPENDIX . . . . .	52
LIST OF REFERENCES . . . . .	62

## List of Figures

Figure 1	Line spread functions of screen-film combinations.	10
Figure 2	Intensity in a sinusoidal image. (a) parameters describing a sine function (b) sine function with 100% modulation (c) sine function with 50% modulation	12
Figure 3	A square-wave intensity distribution. (a) parameters of a square-wave function (b) Fourier spectrum	16
Figure 4	Crenelate lead test pattern.	22
Figure 5	Computer display of microdensitometer scan data (primary image).	26
Figure 6	Microdensitometer scan of radiograph of lead edge.	28
Figure 7	Relative exposure versus position in the primary image of a sharp lead edge.	30
Figure 8	MTF of the primary imaging procedure.	32
Figure 9	Components of a typical image intensifier-television fluoroscopic system.	34
Figure 10	Microdensitometer scan of photograph from television monitor screen.	36
Figure 11	Relative exposure versus position in the television monitor image of a crenelate test pattern.	37
Figure 12	Overall MTF of the IITS.	38
Figure 13	Oscillograph of composite video image of square-wave pattern.	40
Figure 14	MTF measured from composite video.	42

Figure 15	MTFs of components of an imaging system	44	vii
Figure 16	Line selection and identification device	54	
Figure 17	Composite video signal	56	
Figure 18	Schematic diagram of line selection and identification circuits	59	

## CHAPTER I

### INTRODUCTION

The application of x-rays to diagnostic medicine rapidly followed their discovery by Roentgen in 1895. Early the next year the use of radiography in location of foreign metallic objects in patients was described (1). The development of fluoroscopy began in November of 1896 when MacIntyre (2) replaced the radiographic film with a fluorescent screen. This eliminated the necessity of waiting for photographic plates to be processed and allowed the physician to view dynamic physiological activities within the patient.

In his classic Carmen lecture of 1941, Chamberlain (3) described the state of fluoroscopy at that time. In doing so, he discussed the limitations of fluoroscopy which, if overcome, would revolutionize diagnostic radiology.

#### Limitations of conventional fluoroscopy

The chief limitation of conventional fluoroscopy was that the energy of the radiation transmitted by a patient under examination, when converted into light, was insufficient to produce a bright diagnostic image. Although an image could certainly be seen, it was only by means of the scotopic or rod vision of the dark-adapted eye. The eye in such a state has poor visual acuity because of the low density of active photoreceptors at low light levels. (Chamberlain's paper contains an excellent review of retinal physiology with reference to acuity and dark-adaptation.) Because of this, diagnostic information, although present on the fluoroscopic screen, could not be detected by the eye.

### Need for an increase in image brightness

An increase in fluoroscopic brightness was desirable and an obvious method of achieving this was to increase the total energy incident on the fluoroscopic screen by increasing the current in the x-ray tube or by decreasing the focal spot-film distance. Unfortunately either of these procedures would result in an increased exposure rate at the patient's skin. A typical exposure rate at the skin at that time (3) was 30 Roentgens/minute, and as the harmful effects of radiation on biological material were already well known, an increase was considered inadvisable.

If exposure rate could not be increased, the alternative was to attempt to improve image brightness by making more effective use of the x-rays transmitted by the patient. It was established that to take advantage of the highly acute photopic vision, a brightness gain of at least 1000 times was required. Since it was known that the conventional fluorescent screen was about 3% efficient, and, therefore, that an ideal screen could only offer an improvement of about 33 times, it was concluded that an amplification device was necessary to obtain the required gain.

### The image amplifier

Vacuum-tube image amplifiers were developed by Langmuir at General Electric ca. 1938 and by Coltman (4) at Westinghouse Laboratories in 1948. The Coltman design which is employed in most modern

image amplifiers consisted of a zinc sulphide input phosphor surface which absorbed x-ray photons and produced a deep-blue-near-ultraviolet light image. The light from this phosphor became incident upon an adjacent cesium antimony photocathode which produced photoelectrons. These electrons were accelerated across the vacuum tube by a high potential difference and focussed to impinge on a zinc cadmium sulphide output phosphor to produce a visible image. A brightness gain resulted both from the external energy given to the electrons by the potential difference, and from a geometrical minification of the image on the output phosphor which increased the density of light photons.

Coltman's early tubes had an electronic brightness gain of 5-20 times and a minification ratio of 25 (5 diameters). The overall gain of such tubes, therefore, varied from 125-500 times.

Coltman predicted that an image tube coupled to a television chain could offer sufficient brightness for photopic viewing, plus the versatility of a television output.

#### Present state of fluoroscopy

This pioneer research has resulted in the development and acceptance of modern image intensifiers for routine use in gastrointestinal and cardiac fluoroscopy. Such intensifiers have been coupled to vidicon, image orthicon, and plumbicon television cameras, and to spot film and ciné recording cameras to form complete image intensifier fluoroscopic

systems. The fluoroscopic image can be viewed on a local or remote television monitor and can be recorded on tape or film for reference or teaching.

Technical innovations in fluoroscopy such as automatic image brightness regulation, large input field light amplifiers, or the high quantum efficiency cesium iodide input phosphor are continually being introduced.

#### Need for image evaluation

It is essential in the operation of a diagnostic radiology department to ensure that the available equipment is producing the best diagnostic image possible within exposure rate restrictions. To do this it is necessary to have a method for evaluating the performance of diagnostic imaging equipment. This is not such a straightforward problem as it would at first appear.

The term "image quality" used with reference to fluoroscopy cannot be described by a single variable. Johns (5) uses the five terms: "brightness", "contrast", "unsharpness", "resolution", and "noise" as components necessary to specify image quality fully. Furthermore, there is a certain amount of interdependence among these variables. Because an imaging system could rate highly in one quality component but poorly in another, it is often difficult to make comparisons between different systems and conclude that one is better than another.

This problem did not exist with a conventional fluoroscopic unit consisting of merely an x-ray machine and a fluorescent screen. For a

given patient or phantom in the beam and a given kilovoltage, tube current, and filtration, the performance of the screen was fully described by its light output or brightness and its resolution. The resolution of a fluorescent screen was dependent only on the size of its phosphor particles which did not vary in time. Measurements or comparisons of light output were simple, requiring only an ion chamber and a photometer (6). The other variables of image quality depended on the x-ray tube and patient rather than on the imaging system.

In comparison, the evaluation of a multicomponent imaging system is much more difficult. There are no less than four methods of varying the output brightness, without changing the exposure rate. There are several stages at which noise is introduced, and where unsharpness or resolution are affected. Contrast can be electronically controlled at the television monitor. In order to produce a high quality diagnostic image, all of the variables must be optimized. The effects of each control on overall image quality must be analyzed.

This brief review of the development of the science of fluoroscopy has attempted to show the great increase in complexity of fluoroscopic equipment and the resulting need for more sophisticated methods of measuring the performance of this equipment. It is the purpose of the work described here to attempt to develop such a method.

In the following chapters the various methods of measurement of image quality will be described and an attempt will be made to justify the use of the Modulation Transfer Function as a means for specifying the

performance of fluoroscopic systems. The Modulation Transfer Function of an image intensifier television fluoroscopic system under actual operating conditions will be measured and a comparison will be made with results obtained by another method.

## CHAPTER II

### METHODS OF IMAGE EVALUATION

7

The image intensifier television system (IITS) is basically a combination of electron-optical and visible light imaging components. In seeking a method of evaluating image quality one can, therefore, utilize the results of many years' research in the photographic and optical sciences. Many such methods have been introduced in the literature and with some adaptation, these have been applied to radiological evaluation (7, 8, 9).

#### Subjective methods

Methods of image evaluation can be divided into two categories; subjective and objective. Subjective methods, as the name implies, take into account the visual response of the observer making the test. These tests generally make use of wire mesh(10, 11, 12), bar or wedge (11, 13, 14) resolution phantoms or contrast detail phantoms (12, 15, 16, 17, 18). They are useful because they can be conducted fairly rapidly and inexpensively and can supply semi-quantitative measurements of image quality. Furthermore, since the process of diagnosis involves several physiological and psychological factors of human vision and perception, the incorporation of a human observer as a measuring instrument has a rational basis.

Unfortunately, it has been shown (12) that results of different subjective tests are not mutually compatible; that under certain testing conditions a comparison using two different subjective tests will result

in a reversal of the relative merits of two imaging systems. Another drawback in subjective testing is the fact that there is no satisfactory way to combine the results of subjective image quality measurements of individual components in a multicomponent imaging system into an overall measurement of image quality. Perhaps the greatest difficulty is in variation between observers' opinions of image quality. This makes standardization and comparison of test results almost impossible.

#### Objective testing methods

Line spread function. Objective testing is done by means of a test object, and a scanning detector in the image plane. A common measure of image quality is the line-spread function (LSF) (19). A narrow slit, usually between jaws of heavy metal such as tungsten, lead, platinum, or uranium, is imaged by the system and the intensity of the output as a function of distance in the image plane is recorded. Ideally, the image of a slit would be a line of the same width as the slit (multiplied by the overall magnification or minification of the imaging system). However in practice there is unsharpness introduced by the imaging procedure which causes the output to be blurred or spread, hence the name line-spread function.

Any object varying in x-ray opacity along one dimension can be considered as an infinite set of adjacent parallel line sources of radiation incident on the imaging system. When such an object is imaged,

the image of each line is found by multiplying its intensity by the LSF. The output of the object is just the superposition of the line images. This process is known as convolution (20).

The line spread function describes the unsharpness characteristics of an imaging system by uniquely predicting the output for any one-dimensional input. Because of this, it is called a transfer characteristic for one dimensional information.

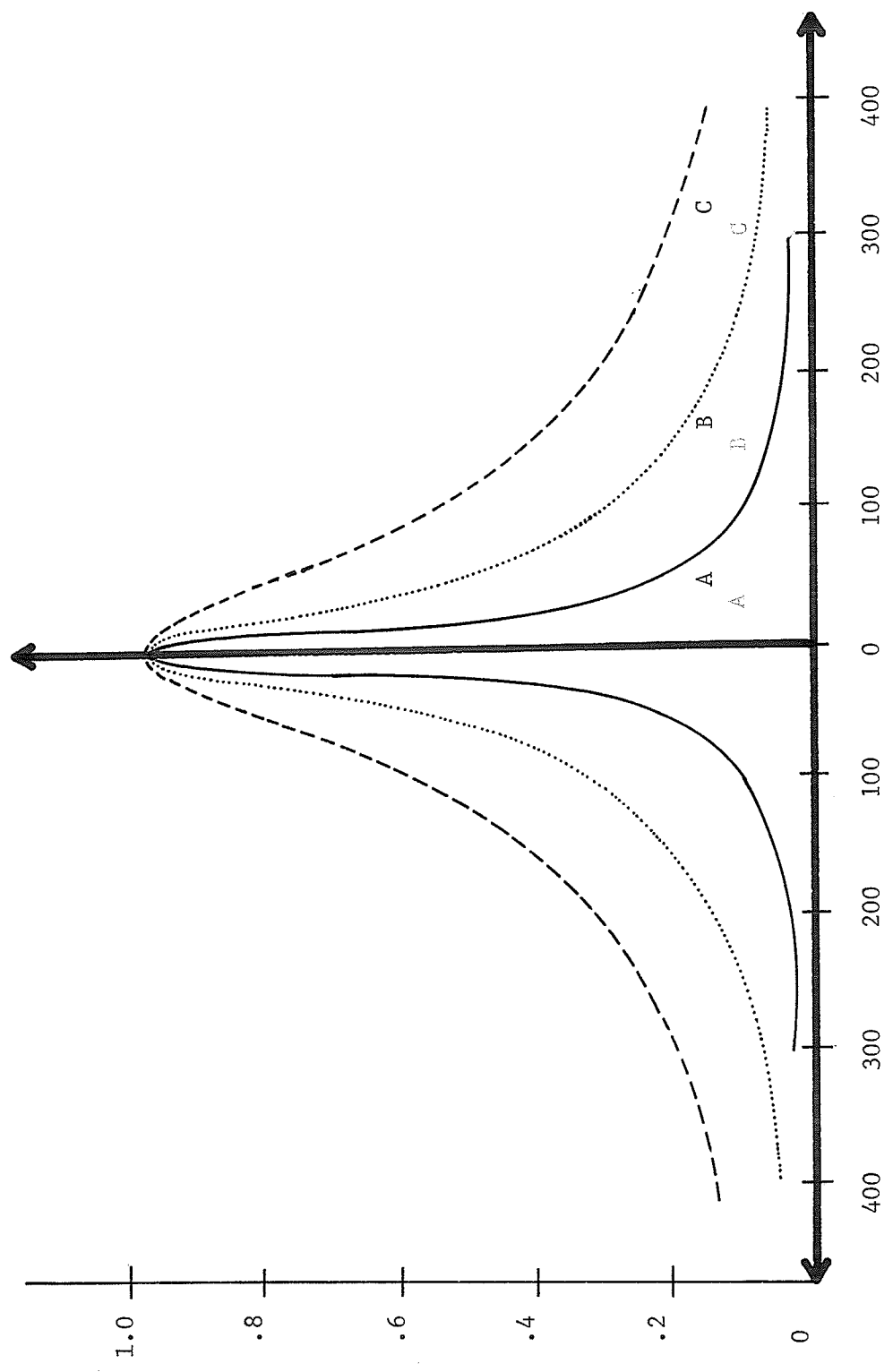
A set of line spread functions is shown in Figure 1. These are used in radiography for assessing screen-film combinations. It is seen that the narrower the line spread function, the less unsharpness introduced and the higher the definition of the system.

The main disadvantage with the LSF is in evaluating multicomponent systems. In order to combine the unsharpness characteristics of several components, a multiple convolution of each of their line spread functions must be performed. This is extremely difficult in practice and limits the suitability of the LSF for this purpose.

Modulation transfer function. When an object is placed in an x-ray beam a distribution of transmitted radiation corresponding to variations in its radio-opacity is formed. This is referred to as the "primary radiological image" (5).\* For present purposes its intensity is measured in terms of photon fluence, exposure, or exposure rate.

If the intensity of the primary image formed at the plane of the input to the imaging system under test varies sinusoidally in space

\*Hereafter referred to as the "primary image". See Figure 9, Page 34.



DISTANCE (microns)

FIGURE 1

LINE SPREAD FUNCTIONS OF RADIOGRAPHIC

SCREEN-FILM COMBINATIONS

- A. Slow speed, high definition
- B. Medium speed, medium definition
- C. High speed, low definition

along one dimension, and is constant in the orthogonal dimension in the plane, then it can be described by the equation

$$F(x) = F_0 + F_1 \sin 2\pi fx \dots \dots \dots (1)$$

where  $F(x)$  is the intensity of the primary image,  $F_0$  is the mean value of the intensity,  $F_1$  is the amplitude of the sinusoidal variation, and  $f$  is the spatial frequency (Figure 2a).

Modulation is defined as the ratio of the amplitude to the mean value of the intensity.

$$M_i = \frac{F_1}{F_0} \dots \dots \dots (2)$$

The concept of modulation is illustrated in Figure 2 (b and c). Since intensities, by definition, are always positive, the value of the modulation cannot exceed 100%.

It has been shown (7, 8) that when a sinusoidal input is imaged by a system, the convolution of the sine function with the line spread function of the system results in a sinusoidal output intensity\*

$$G(x) = G_0 + G_1 \sin 2\pi(mf) x \dots \dots \dots (3)$$

where  $m$  is the lateral magnification of the imaging system, assumed constant over the entire image plane.

The magnification or minification of the system causes the spatial frequency of the image to be decreased or increased by a factor  $m$ .

\* For a derivation of this see appendix B page 65

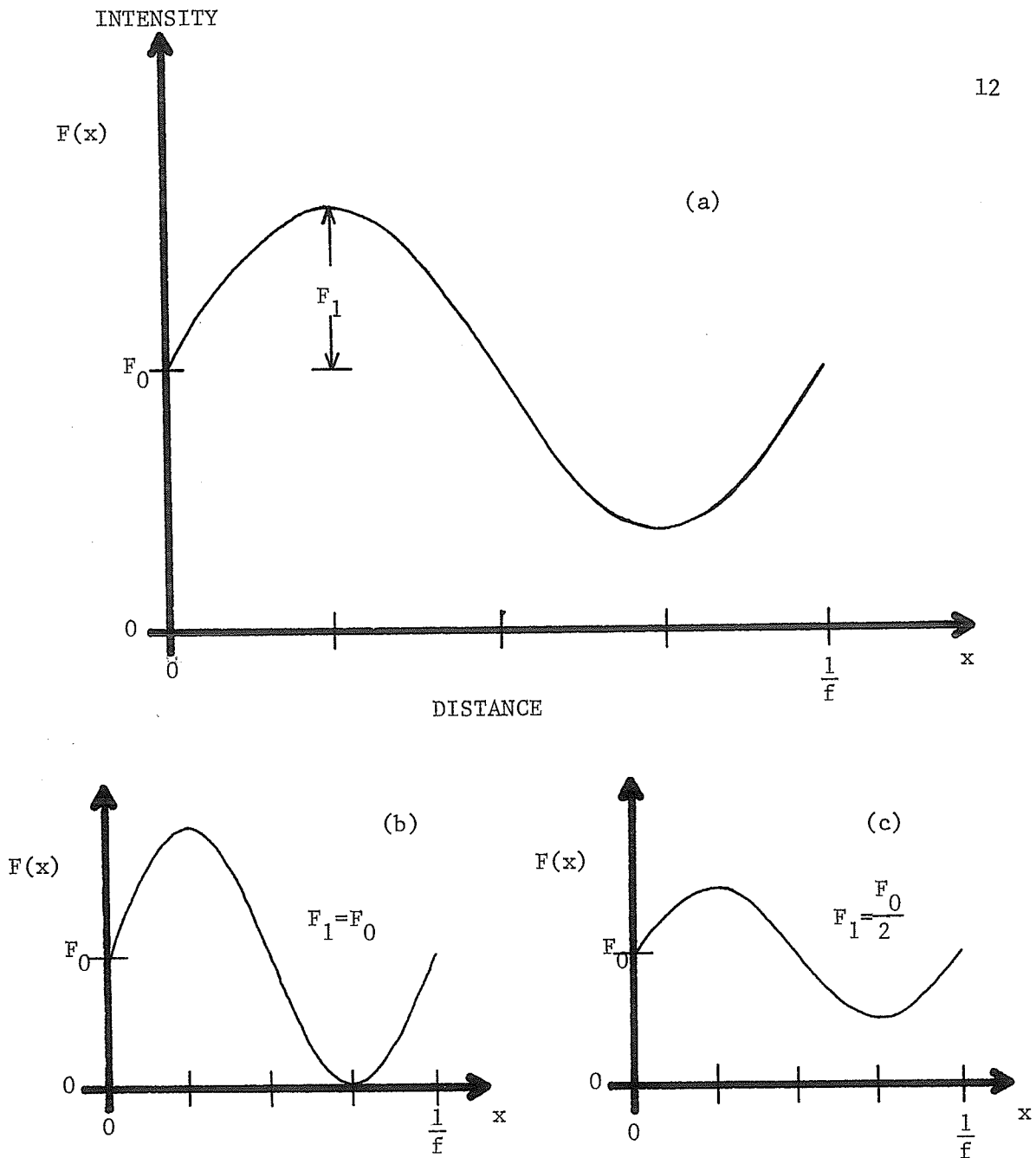


FIGURE 2

## INTENSITY IN A SINUSOIDAL IMAGE

- (a) parameters describing a sine function
- (b) sine function with 100% modulation
- (c) sine function with 50% modulation

Equation 3 can be rewritten in terms of the input parameters as

$$G(x) = A \{ F_0 + T_f F_1 \sin 2\pi(mf) x \} \quad \dots (4)$$

The output intensity is modified by two factors; A, the overall amplification of the imaging chain, and  $T_f$ , the amplitude transfer factor. The frequency dependence of the system in transmitting sine waves is contained in  $T_f$  which, in general, decreases with increasing frequency (7, 8, 9). In a perfectly faithful imaging system,  $T_f$  would have a value of one at all spatial frequencies, and the input and output would differ only by the frequency independent factor A.

The modulation of the output intensity is given by

$$M_0 = \frac{A T_f F_1}{A F_0} = \frac{T_f F_1}{F_0} \quad \dots \dots \dots (5)$$

The modulation transfer factor is defined as the ratio of output and input modulations.

$$MTF = \frac{M_0}{M_i} = \frac{T_f F_1 F_0}{F_0 F_1} = T_f \quad \dots \dots \dots (6)$$

This factor is the sine wave response of the system at the spatial frequency f.

It is possible, at least theoretically, to image a series of sinusoidal inputs, each of a different spatial frequency, and measure the modulation transfer factors for each. A graph of modulation transfer factor versus spatial frequency is known as a modulation transfer function. It is analogous to the sine wave response of an

acoustical system.\*

The modulation transfer function (MTF) describes resolution and unsharpness in terms of the sine wave response. Because it is a response function in spatial frequency space rather than a spread function in Cartesian space, it is possible to obtain the MTF of a system of cascaded components very simply when the individual MTFs are known. The overall MTF is found by point by point multiplication of the individual MTFs.\*\*This is much easier to do than the multiple convolutions described with reference to the line spread function.

The "resolution" describes the spatial frequency in number of line pairs per millimeter, at which the response has fallen off to some (subjective) threshold value; i.e. the maximum spatial frequency at which an observer perceives a transmitted image. This represents only one point on the response curve of the system. An obvious advantage of using the MTF is that the ability to image many spatial frequencies is measured. Diagnostic radiologic information contains diffuse as well as fine-detailed regions and imaging performance should be judged over the entire range of spatial frequencies.

\*In many imaging systems there is a phase shift of the sine waves from input to output. The dependence of phase shift on spatial frequency is described by the "phase transfer function". This combined with the MTF yields the optical transfer function (OTF). In this work only MTF will be discussed.

\*\*System linearity is assumed throughout this analysis. The validity of the MTF as a response or transfer function is shown by Rossman et al. (36).

Practical measurement of MTF

In practice it is extremely difficult to produce test objects that generate a primary image that is sinusoidal and such an object if constructed would be useful at only one x-ray quality. Measurement of MTF by straightforward means, although possible in optics, is seldom attempted in radiological evaluations. Instead, indirect methods are employed.

Bouwers (21) and Moseley (22) used a device consisting of two line grids rotating with respect to one another to generate moiré patterns. The primary image produced by this arrangement approximated sine waves of varying spatial frequencies.

Another means of obtaining sinusoidal information from non-sinusoidal objects involves the use of the Fourier analysis technique. A brief review of this is in order.

Fourier analysis. The Fourier theorem states that any piecewise continuous periodic function  $F(x)$  can be synthesized as a superposition of sine functions of appropriate amplitudes and frequencies.

$$F(x) = F_0 + \sum_{n=1}^{\infty} F_n \cos 2\pi nfx \quad \dots \dots \dots (7)$$

where the  $F_n$ s are called Fourier amplitudes and are given by

$$F_n = f \int_0^{\frac{1}{f}} F(x) \cos 2\pi nfx \, dx \quad \dots \dots \dots (8)$$

For a square wave of period  $\frac{1}{f}$  such as is shown in Figure 3a

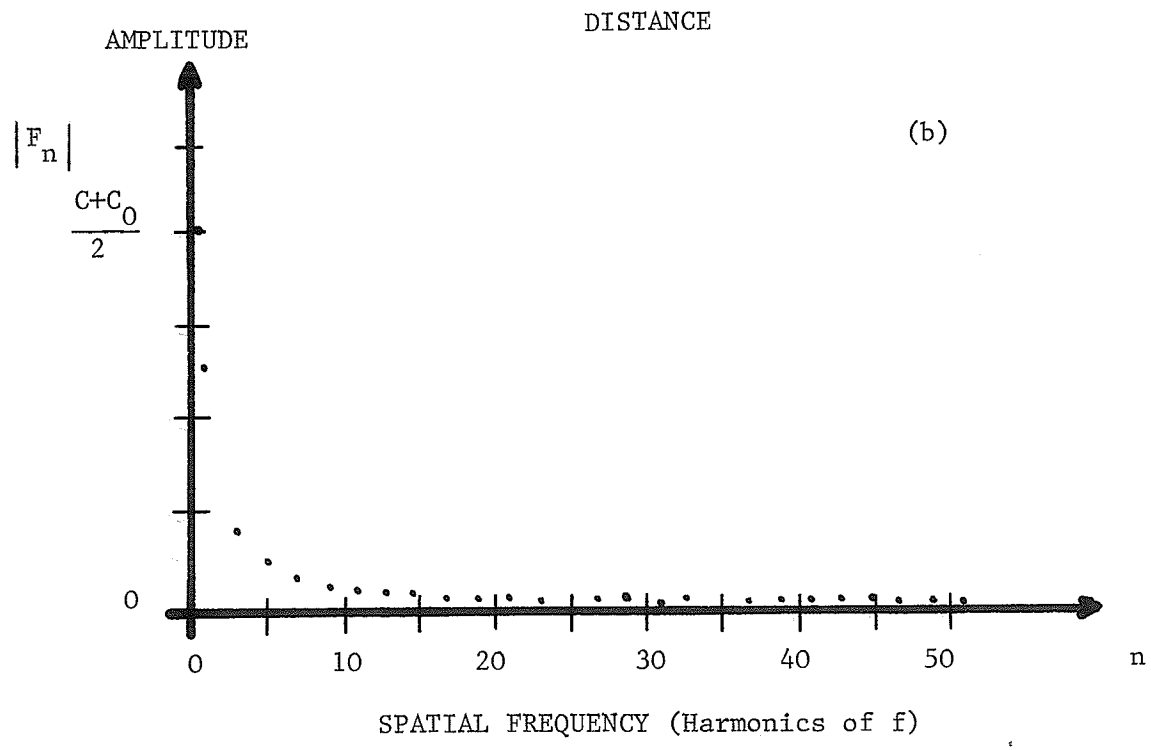
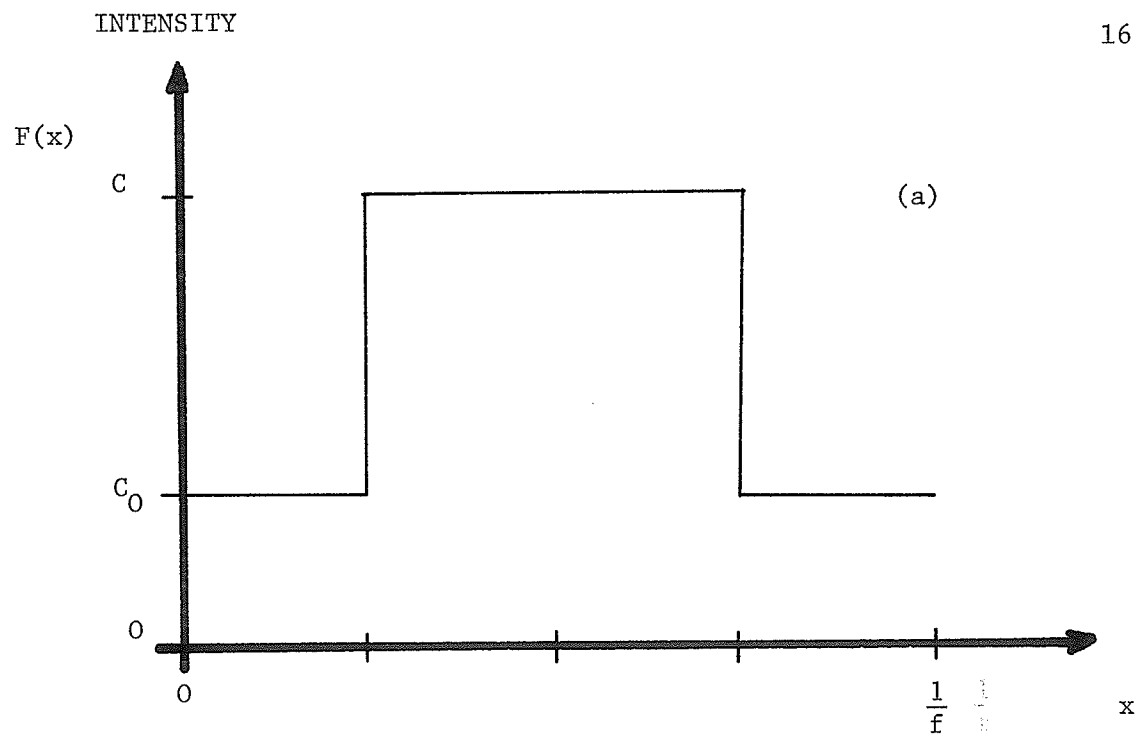


FIGURE 3  
A SQUARE-WAVE INTENSITY DISTRIBUTION  
(a) Parameters of a square-wave function  
(b) Fourier spectrum

$$\begin{aligned}
 F(x) = & \begin{aligned} & C_0 \text{ when } 0 \leq x \leq \frac{1}{4f} \\ & C \text{ when } \frac{1}{4f} < x < \frac{3}{4f} \quad \dots \dots \dots (9) \\ & C_0 \text{ when } \frac{3}{4f} \leq x \leq \frac{1}{f} \end{aligned}
 \end{aligned}$$

the Fourier amplitudes are

$$\begin{aligned}
 F_n = & \begin{aligned} & \sin \frac{n\pi}{2} \frac{C-C_0}{n\pi} \quad (n \neq 0) \\ & \dots \dots \dots (10) \\ & \frac{C+C_0}{2} \quad (n = 0) \end{aligned}
 \end{aligned}$$

The graph of these Fourier amplitudes versus spatial frequency is shown in Figure 3b. Thus a square wave is composed of an infinite number of sine waves whose frequencies are odd multiples of the fundamental frequency  $f$  of the square wave and whose amplitudes are inversely proportional to the harmonic number  $n$ .

The procedure for obtaining the Fourier amplitudes from the spatial representation of the function  $\{F_n \text{ from } F(x)\}$  is called Fourier transformation. Equation 8 is said to be the Fourier transform of Equation 7.

Application of Fourier theory. It is relatively easy to produce a crenelate pattern whose primary radiological image intensity obeys Equation 9. According to Fourier theory the imaging of this pattern is equivalent to imaging an infinite number of sine waves.

Moseley (23) used a 50 micron thick lead foil (of a type often used for subjective measurements) containing a series of square waves of different spatial frequencies, and measured the square wave response of image intensifier television systems with a variety of television camera tubes.

Since the dominating Fourier component of a square wave is a sine wave of the same frequency (see Equation 10), the square wave response measured is approximately equivalent to the MTF. The frequency response measured by this technique is called the contrast transfer or contrast frequency response function (5). For each spatial frequency at which the response is measured it is necessary to have a square wave of the corresponding frequency.

A frequently used method of obtaining the MTF is to measure the line spread function of the imaging system and calculate the Fourier transform of the LSF (5, 8, 9, 20, 24). The Fourier spectrum of an infinitely narrow line or slit (Dirac  $\delta$ -function) contains equal amplitudes at all frequencies. For radiological purposes a 10 micron slit can be considered to be a line source. Since the spectrum of the input is constant the Fourier spectrum of the image of a slit is, therefore, the modulation transfer function of the imaging system (except for a constant).

In this work we have chosen to make use of harmonics of a single square wave frequency. A crenelate pattern like that in Figure 3a is imaged. The spectrum of sine wave amplitudes in its primary radiological image is obtained by Fourier transformation of the distribution of intensity in the image. The spectrum will differ from that of Figure 3b due to geometrical unsharpness introduced by the finite focal spot size of the x-ray tube (25). The intensity in the primary image can be written as

$$P(x) = F_0 + \sum_{n=1}^{\infty} T_{np} F_n \sin 2\pi n(qf)x \quad \dots \quad (11)$$

where  $T_{np}$  is the transfer factor for sine waves of frequency  $n$  in the primary imaging process and  $q$  is the magnification of this process.

The output intensity distribution can be written as

$$G(x) = A\{F_0 + \sum_{n=1}^{\infty} T_{no} F_n \sin 2\pi n(mf)x\} \quad \dots \quad (12)$$

where  $A$  and  $m$  have the same meaning as in Equation 4.

The modulation in equation 11 is

$$M_{np} = \frac{T_{np} F_n}{F_0} \quad \dots \quad (13)$$

and that in Equation 12 is

$$M_{no} = \frac{A T_{no} F_n}{A F_0} = \frac{T_{no} F_n}{F_0} \quad \dots \quad (14)$$

The modulation transfer factors are given by

$$\text{MTF} = \frac{M_{no}}{M_{np}} = \frac{T_{no} F_n}{F_0} \frac{F_0}{T_{np} F_n} = \frac{T_{no}}{T_{np}} \quad \dots \quad (15)$$

This is just the ratio of the Fourier amplitudes of the output to those of the input. The modulation transfer function is the set of these factors for all  $n$  of interest.

It is customary to express frequency response in terms of inverse distance in the plane of the object. For this reason, magnifications can be ignored in response calculations since a spatial frequency of  $mf$  in the image plane for example merely refers to a frequency  $f$  in the object plane. Since only one square wave frequency is used, this does not lead to confusion.

The total diagnostic fluoroscopic process can be divided into three functional units. Each of these introduces a certain amount of deterioration into the diagnostic image. The units are: (1) the x-ray machine and the patient, (2) the image intensifier television system, and (3) the radiologist and viewing conditions under which he works. In evaluating an image intensifier television system it is essential to isolate those factors that the system contributes to the total deterioration from those due to (1) and (3).

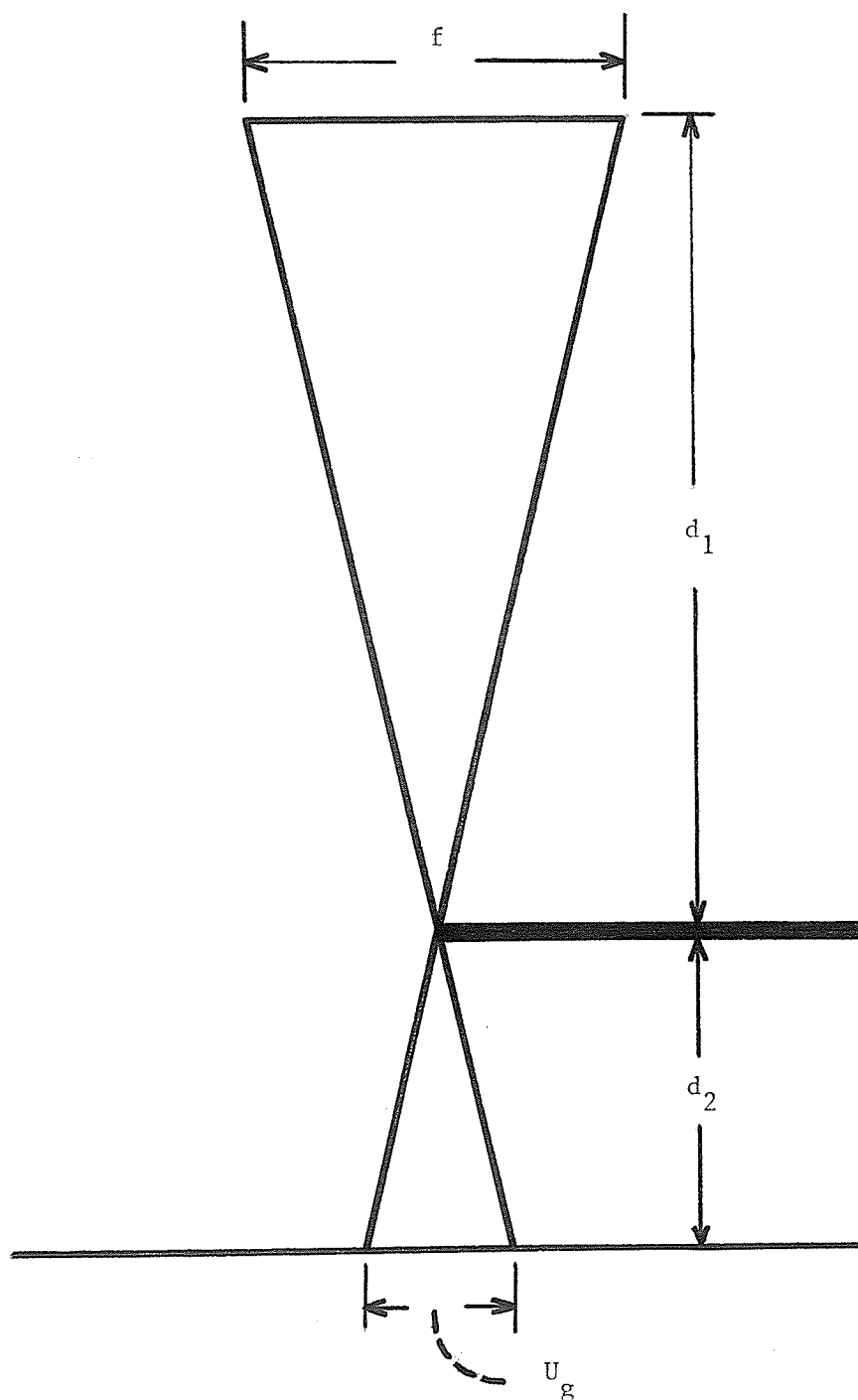
The physiological and psychological effects of a human observer and variations between observers are eliminated by using an objective evaluation method. The factors associated with the x-ray geometry and the patient are controlled by careful design of the test object and experimental arrangement.

#### The square wave test pattern

The finite size of the x-ray focal spot causes sharp edges in the object to be blurred in the primary image. In order to produce a primary image that is as close as possible to a square wave, it is desirable to minimize this blur. Unsharpness due to focal spot size is expressed by the equation

$$U_g = \frac{f d_2}{d_1} \dots \dots \dots (16)$$

Here  $f$  is the effective focal spot size,  $d_2$  is the separation between the plane of the object and that of the primary image and  $d_1$  is the focal spot-object distance.  $U_g$  is the width of the penumbra in the image plane of the image of a sharp edge. See next page.



GEOMETRICAL UNSHARPNESS DUE TO FINITE FOCAL SPOT SIZE

Geometrical unsharpness is minimized by making  $d_1$  as large as possible and  $d_2$  as small as possible. The unit used for development of a testing procedure was a Picker Therapy Simulator with a large field Delcalix light amplifier and an image orthicon television pickup. The focus-object distance was adjustable over a wide range.

The test object was placed on the input phosphor of the Delcalix so that  $d_2$  was less than one centimeter. The value of  $d_1$  was set at 135.5 cm. so that for a 2 mm focal spot  $U_g$  is less than .015 mm. The test pattern was constructed of lead so that for a reasonable absorption of radiation it would be thin enough to be considered two dimensional. This minimized unsharpness as well as reducing the Compton scatter volume of the pattern. A sketch of the pattern is shown in Figure 4. A 9 inch square sheet of lead was rolled and milled to a thickness of .75 mm.

Along one dimension of the sheet three grooves 25.4 mm wide separated by 25.4 mm were milled .15 mm into the lead. For rigidity and protection the lead was mounted on a thin sheet of plexiglass with double-backed tape and coated with lacquer. The absorption of 90 kilovolt radiation by the pattern approximated that of a human abdomen.

#### Input to the imaging system

The primary image produced by the test object is the input to the imaging system under test. In order to determine how closely this image resembles a perfect square wave, the MTF of the primary imaging procedure must be measured.

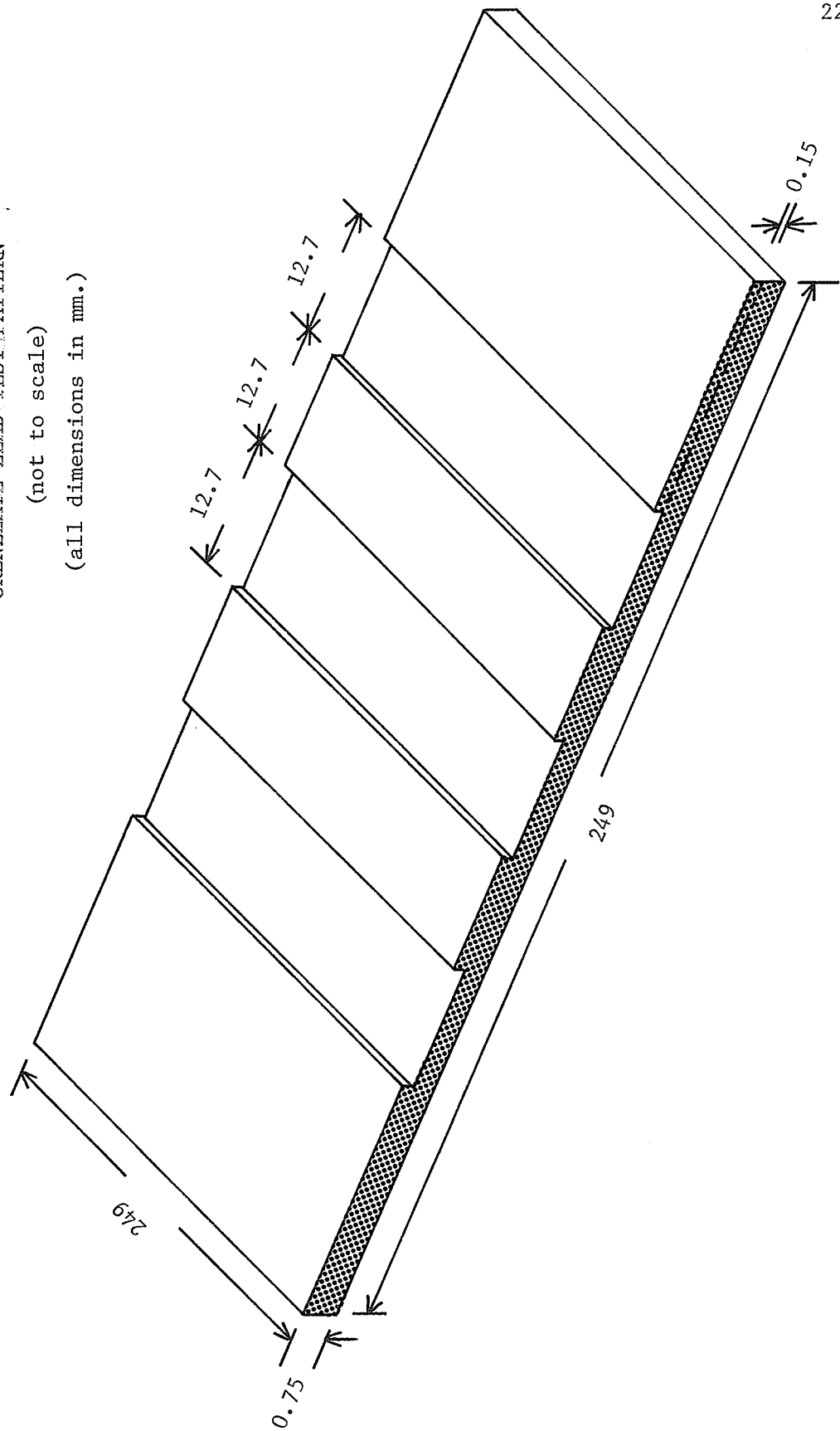
The frequency response of the primary imaging procedure determines

FIGURE 4

CRENEULATE LEAD TEST PATTERN

(not to scale)

(all dimensions in mm.)



how sharp the image of a sharp transition in the square wave will be. This is because the sharpness of an edge depends on the presence of high frequency Fourier components. A decline in frequency response causes "corners" to be rounded off in the image. Therefore, in MTF measurements we are chiefly interested in edge response; the flat top and bottom of the square wave being used chiefly to define the boundaries of this region. The use of edges to characterize a square wave will be dealt with in the following sections.

Because of its excellent fine-grain characteristics Kodak Type M Industrial X-Ray Film was used to record exposure in the primary image plane. The film was enclosed in a cardboard cassette placed on the input phosphor of the intensifier. A sheet of lead, 3.18 mm. thick was placed over half of the film so that the image of a sharp edge of the lead would be radiographed. The edge was located approximately on the central axis of the x-ray beam. An exposure of 500 milliamperes-seconds at 90 kilovolts was made. At this exposure, virtually no radiation could penetrate the lead although the portion of the film not covered by the lead received an adequate amount of radiation to produce an average optical density of 1.15.

Type M film is very insensitive to direct x-radiation. To produce a similar optical density with the test pattern described in the last section would have required an exposure over twenty-one times as great. This is quite time-consuming since the x-ray tube must be allowed to cool after each five second exposure or the anode might be damaged. Since it is the edge response that is to be measured, either test object can be

used with equivalent results.

The film was developed for eight minutes in standard x-ray solutions at 72° F, fixed, washed, and dried. A portion of the negative containing the image of the edge was excised and mounted on a microscope slide.

#### Microdensitometry

The slide was scanned on a Zeiss 05 Scanning Microscope Photometer under a magnification of 576. Oil immersion microscopy technique was observed. A Digital Equipment PDP12 computer controlled the scanning stage and the acquisition of data. A photomultiplier measured the transmission of light from a tungsten lamp through the negative. The microdensitometer was arranged to record a maximum of 127 points per scan. The distance between observation points could be specified as an integral multiple of 0.5 microns. In order to measure the transmittance of the film in the region of the edge with sufficient detail, but to have a large enough scanning range to include the flat top and bottom outside the transition region, a step of 12.5 microns was chosen. The direction of the scan was aligned perpendicular to the edge. A rectangular measuring aperture defined the photomultiplier input field for each scanning step. The aperture was adjusted so that the input fields for each step were adjacent but not overlapping. Since the width of the step was 12.5 microns and the measuring aperture occupied a plane on which the image was magnified 576 times, the aperture was set to 7.2 mm. in the direction parallel to the scan. The 12.5 micron step size created a sampling error in the MTF of less than .005 (37).

The computer printed out the scan data as a series of percentage transmission values. The computer c.r.t. display of a typical scan is shown in Figure 5. The transmission values were calculated relative to an arbitrary point on the negative but their scale was linear.\*

To convert the relative values to an absolute scale standard densitometry was used. Average values of the optical density of regions on the negative on either side of the edge were obtained. Care was taken to sample far enough from the edge to be beyond the penumbra effect. The optical densities were converted into absolute transmittances by the relation

$$T = 10^{-\text{(O.D.)}} \dots \dots \dots (17)$$

If the transmittance on the dense region of the negative (exposed with no lead) is  $T_1$  and the transmittance on the light region of the film (exposed through 3.18 mm of lead) is  $T_2$ , then the linear transformation

$$T = (H-H_1) \frac{(T_2-T_1)}{(H_2-H_1)} + T_1 \dots \dots \dots (18)$$

relates the absolute transmittance  $T$  to the relative transmittance  $H$  measured on the microdensitometer. Here  $H_2$  and  $H_1$  are the average relative values measured on the flat top and bottom of the transmittance

\*Linearity of the photometer is specified by the manufacturer as within  $\pm 0.04\%$ .

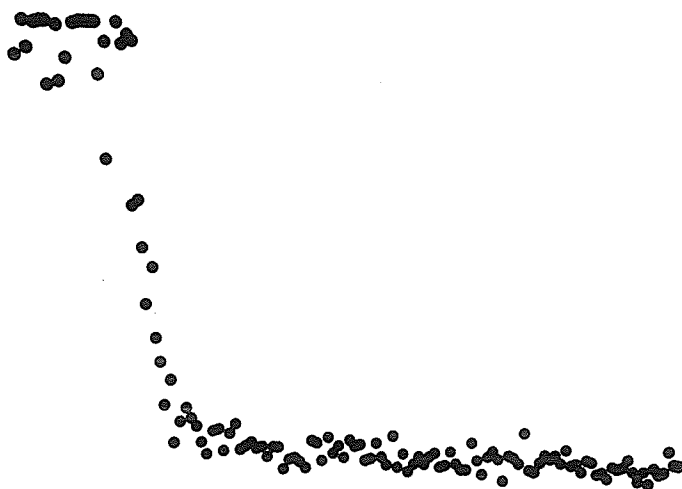


FIGURE 5  
COMPUTER DISPLAY OF  
MICRODENSITOMETER SCAN DATA  
(PRIMARY IMAGE)

distribution.\*

The optical density distribution was calculated by rewriting equation 17 as

$$\text{O.D.} = \log \frac{1}{T} \dots \dots \dots (19)$$

A considerable amount of scatter or noise is seen in the scan of Figure 5. This is largely due to granularity of the film and is especially noticeable where the density is low and clumps of developed silver are sparse. Although granularity often cannot be detected by the naked eye, it creates a problem in microdensitometry. Various remedies employed are to scan the film with multiple parallel slits (30), defocus the microdensitometer slightly (8), or to use a measuring slit that is very long compared to its width. All of these are methods of integrating the measurement in a direction parallel to the edge, along which exposure of the film should be constant. The random fluctuations due to granularity partially cancel and a more accurate measurement of actual transmittance results.

The Zeiss Microscope Photometer has a maximum aperture of 10 mm.. This was extended by making 20 parallel scans across the edge. The effective aperture was then 7.2 mm. by 200 mm.. Figure 6 is a graph of scan data obtained via this technique.

\*The base-plus-fog density on the negative is subtracted from the densities before  $T_1$  and  $T_2$  are calculated. The blackening is then a function of exposure only.

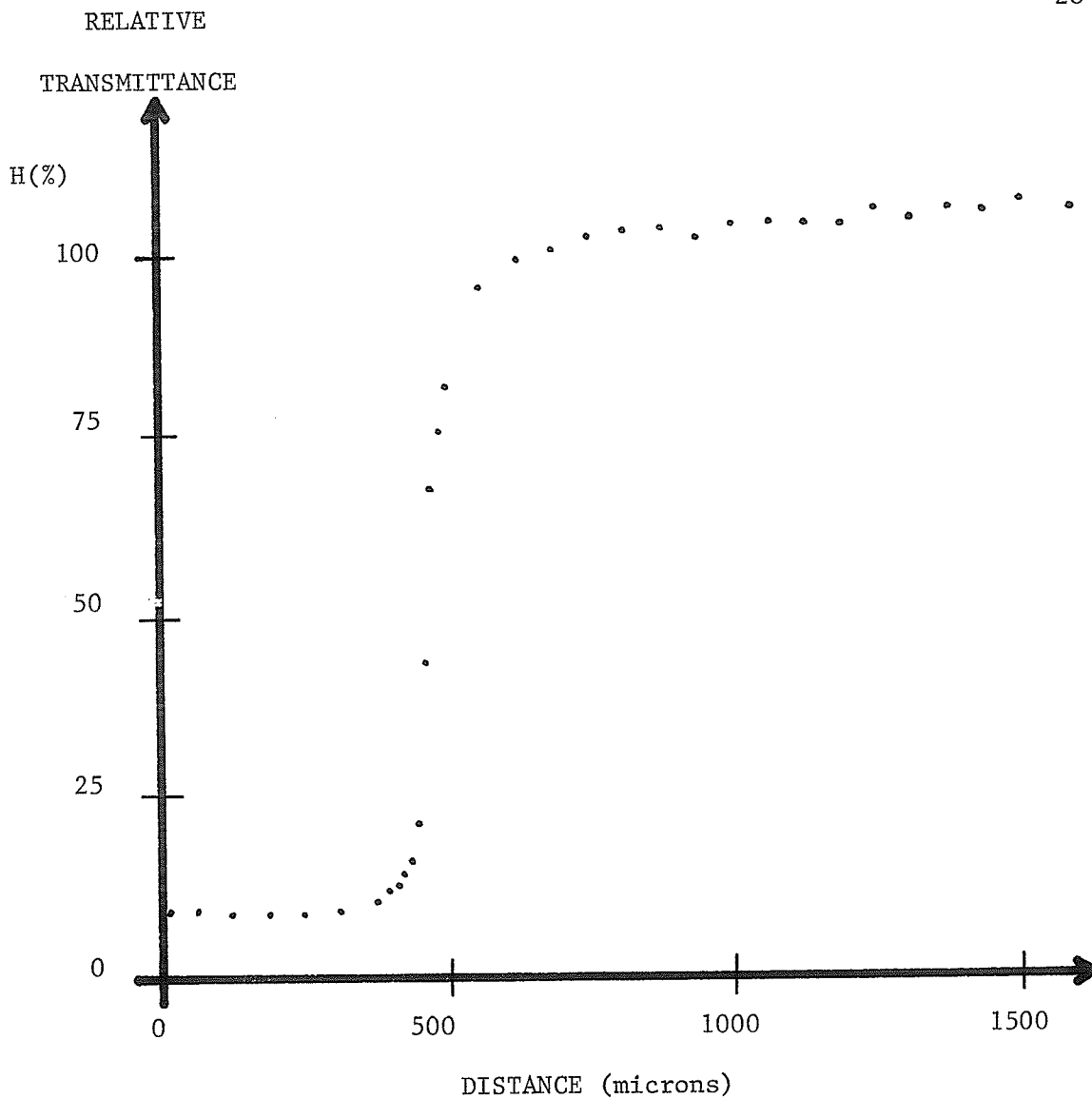


FIGURE 6  
MICRODENSITOMETER SCAN OF  
RADIOGRAPH OF LEAD EDGE  
(Average of 20 scans)

### Characteristic curve

The final step in specifying the primary image is to transform the optical density distribution into an exposure distribution. This is done by means of the characteristic curve of the film. For specific processing conditions the characteristic curve relates the optical density to the logarithm of the relative exposure. The curve for Type M film was obtained (26) and values of the relative exposure were calculated. At low densities the density is directly proportional to exposure. The lower part of the characteristic curve was therefore plotted versus relative exposure rather than its logarithm for convenience. A graph of relative exposure versus position in the primary image is shown in Figure 7.

### Calculation of MTF

Thus far the exposure distribution for the primary image of a sharp edge has been obtained. It remains to calculate the Fourier spectrum of the distribution and from it the MTF.

The program FFT42 is based on a discrete Fast Fourier Transform algorithm (27,28,29), and is optimized to run on a CDC-1700 computer. The input to this program consists of a set of data points comprising one cycle of a periodic function. This program was used to calculate and print the Fourier amplitudes of the input waveform. It runs fastest when the number of input points is an integral power of two.

To produce a periodic input, the 127 points of the exposure distribution were fed into the program, a 128th point whose ordinate was equal to the 127th was added and the distribution's reflection about the

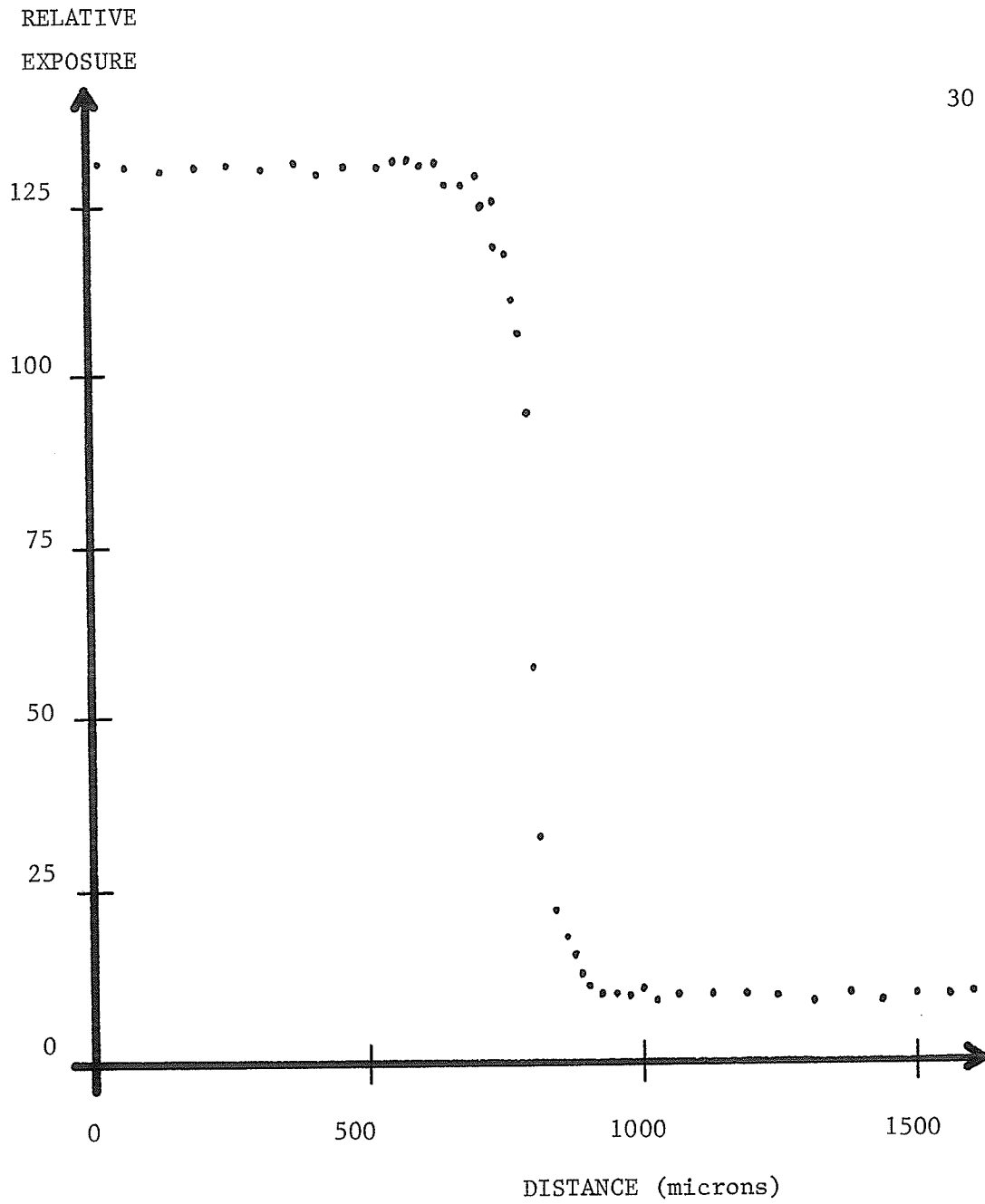


FIGURE 7  
RELATIVE EXPOSURE VERSUS POSITION  
IN THE PRIMARY IMAGE OF A  
SHARP LEAD EDGE

128th point was calculated. Care was taken that the flat top and bottom of the distribution were of the same length. The two arrays were then concatenated. The result of this was that the program received as input a square wave (with rounded-off corners) made up of 256 points. This satisfied the input requirement of periodicity without altering the spectrum of Fourier components being measured.

The output of the program is a 128 point array whose first value corresponds to  $F_0$  in Equation 12. Subsequent values are the  $T_{np} F_n$  of the Fourier spectrum. The modulations are calculated by dividing each  $T_{np} F_n$  by  $F_0$ . This effectively normalizes the spectrum.

The Fourier spectrum of a perfect square wave (Figure 3) is calculated, normalized, and stored in an array in FFT42. Each amplitude corresponds to a value of  $F_n/F_0$  for some particular  $n$ . The MTF is then obtained by dividing the normalized output spectrum by the normalized input spectrum point by point. The MTF of the primary imaging procedure is shown in Figure 8.

#### Measurements on the imaging system

The imaging system of the Picker Therapy Simulator is of the light amplifier type. Between the input phosphor that converts the primary image to light and the photocathode, there is a mirror optical system that collects the light and projects an image of reduced size onto the photocathode. In this way a large area input field can be obtained without encountering the high-cost and engineering difficulties of a large vacuum intensifier.

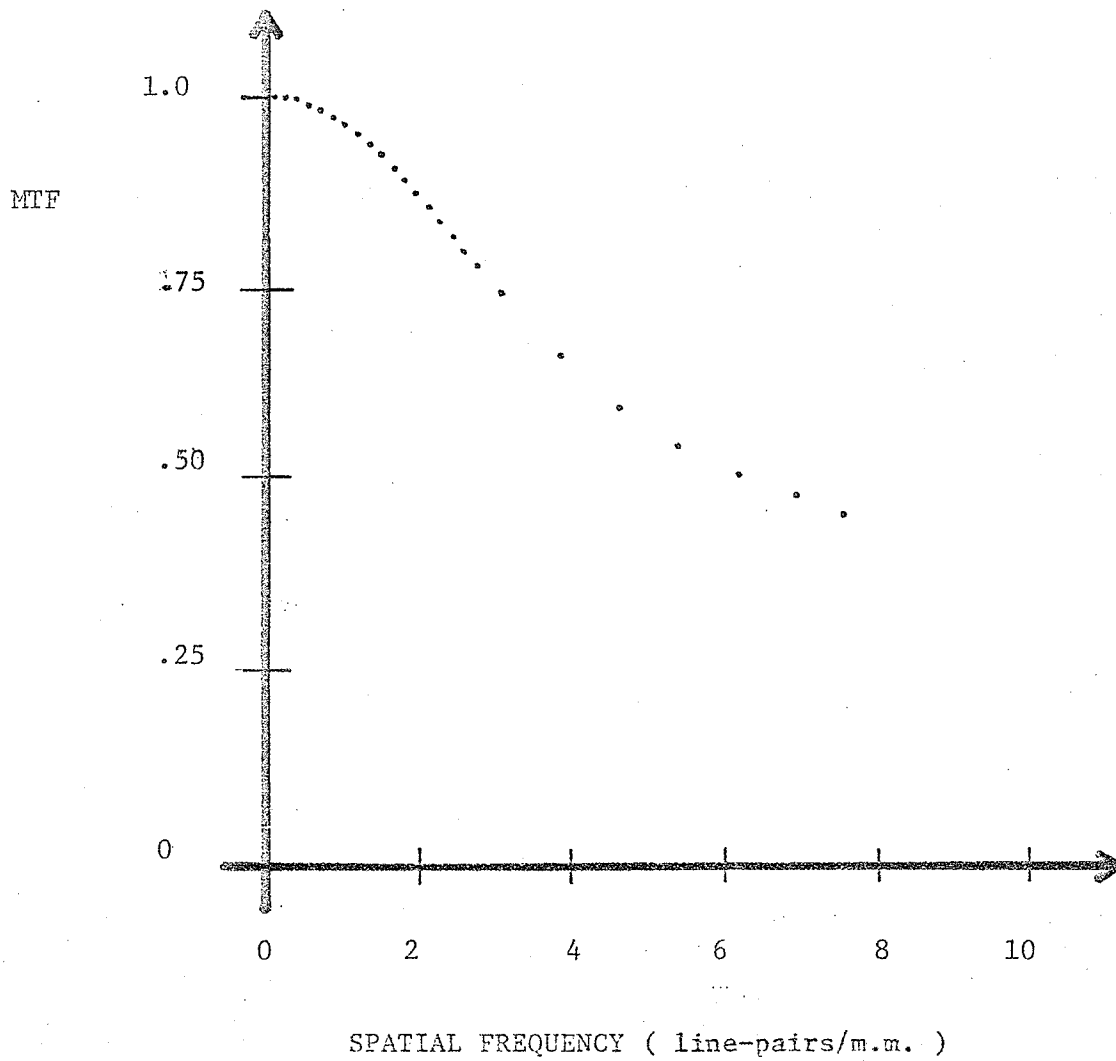


FIGURE 8

MTF OF THE PRIMARY IMAGING PROCEDURE

Figure 9 shows the relationship between the system components and the points at which image sampling is done. Point A is the primary image or input. Measurement of this image was described in the last section. The output of the system is at point C, the television monitor. Point B, the television camera output, is an intermediate location where access to the image for the purpose of evaluation can be gained. The next sections will describe measurements at points B and C.

#### Output of the imaging system

The MTF of the overall imaging process was found from a microdensitometer scan of a photograph of the image on the television monitor formed by x-rays transmitted by the square-wave test pattern. This scan could have been done using the sharp lead edge as a test pattern. However it was considered unwise to operate the intensifier with direct exposure to x-rays because of the possibility of damage to its output phosphor. For this reason, the bar pattern was used.

A considerable change in monitor image quality can be effected by varying the monitor "contrast" and "brightness" settings. For this test, the Simulator operator was asked to set these controls to produce the "best image" that she could. More will be said about this in the Discussion.

Photographs of the television monitor screen were made on 35 mm. Kodak Plus X Pan Film using a close-up adapter on the camera. The same exposure geometry and kilovoltage were used as in measurement of the primary image, except that the x-ray unit was operated in the fluoroscopic mode with a tube current of 5 milliamperes. A camera exposure of 1/30

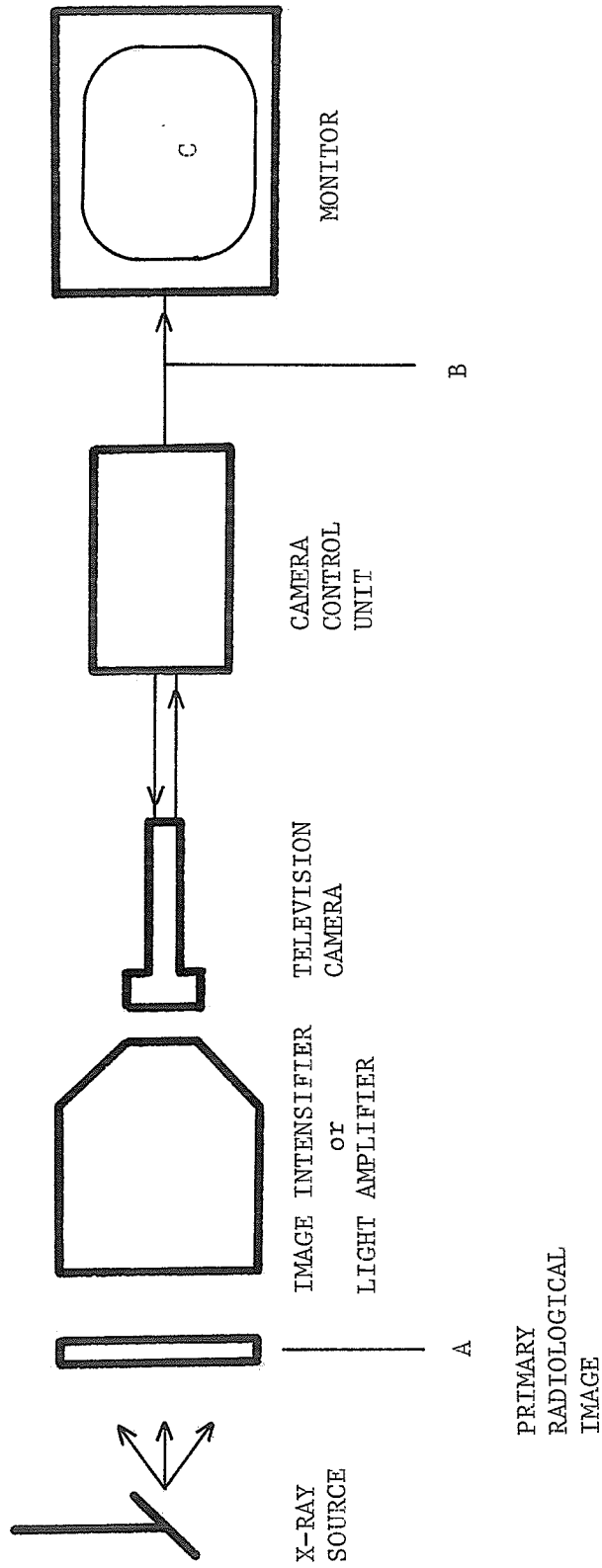


FIGURE 9  
 COMPONENTS OF AN IMAGE INTENSIFIER  
 TELEVISION FLUOROSCOPIC SYSTEM

second with a numerical aperture of  $f/4$  produced a good negative. Development was done in Kodak D 76 developer (1:1) at  $74^{\circ}\text{F}$  for 12.5 minutes. The negative was mounted and scanned as previously described. A graph of the average of 20 parallel scans is given in Figure 10. The absolute optical densities were obtained from the scan data exactly as for the primary image. The conversion to relative exposure, however, was done with the characteristic curve of Plus X film. Figure 11 is a plot of relative exposure versus distance for the television monitor image.

There was a minification of 4.62 times between the primary image and the image on the Plus X film. This was due to the combined minifications of the IITS and the 35 mm. camera. When the MTF is calculated, components of spatial frequency  $4.62 f$  found on the scan of the Plus X correspond to those of  $f$  at the test object on the intensifier. This relationship will hold for all harmonics of  $f$  as well. In order to express frequency response with respect to the object plane (which is almost identical to that of the primary image in this case), the abscissa of the calculated MTF was compressed by a factor of 4.62. The frequency response of the IITS is shown in Figure 12. The MTF values calculated by the program were divided by those of the primary imaging procedure (Figure 8), so that Figure 12 includes only the response of the light amplifier, television camera (an image orthicon in this case), the optical coupling between them, the television monitor, and the measuring apparatus of the experiment. Over the spatial frequency range of interest the MTF of the Plus X, 35 mm. camera, and microdensitometer are nearly one and can be neglected.

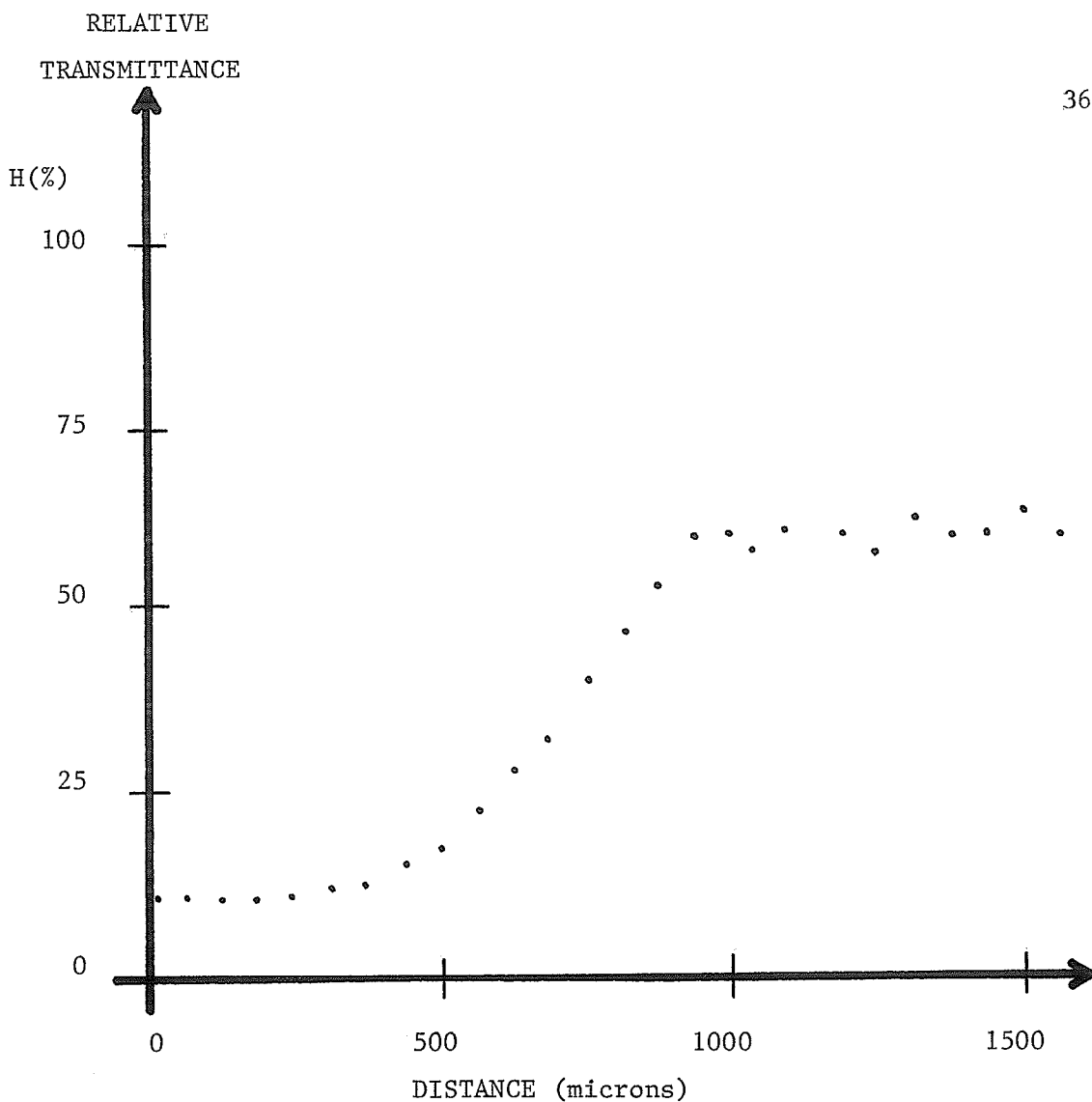


FIGURE 10  
MICRODENSITOMETER SCAN OF  
PHOTOGRAPH FROM TELEVISION  
MONITOR SCREEN

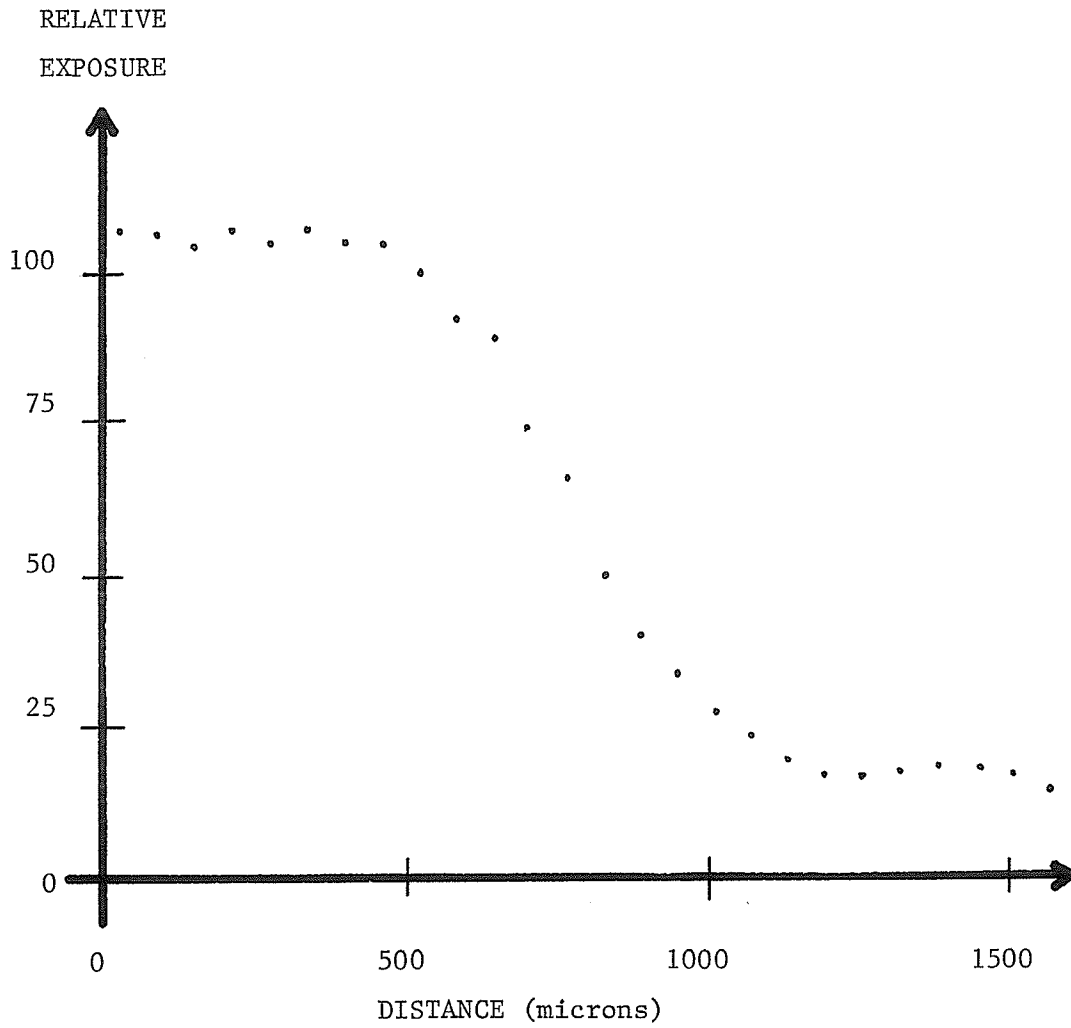


FIGURE 11  
RELATIVE EXPOSURE VERSUS POSITION  
IN THE TELEVISION MONITOR IMAGE  
OF A CRENELATE  
TEST PATTERN

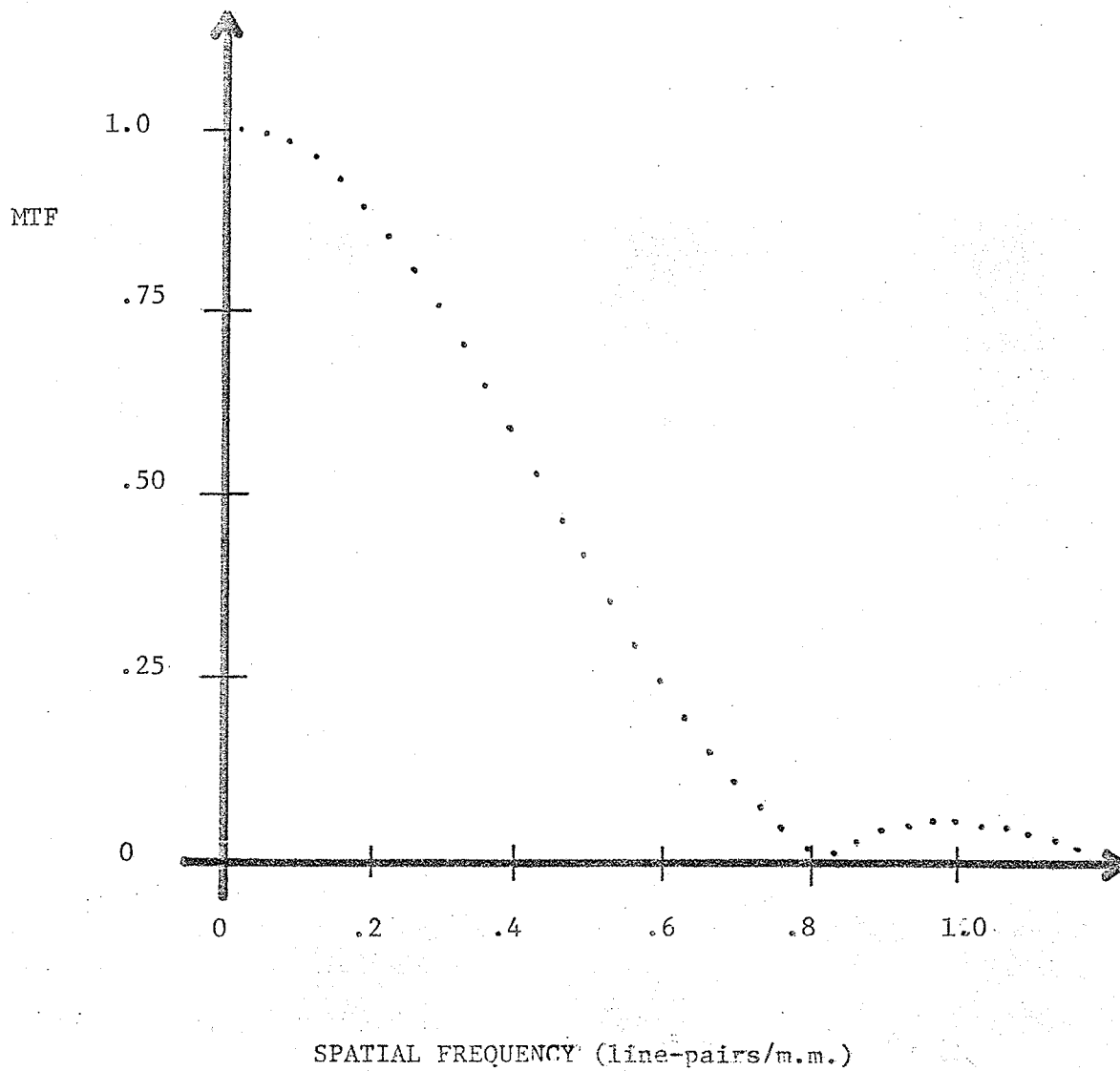


FIGURE 12

OVERALL MTF OF THE IITS

### Output of the television camera

In most image intensifier television systems the output of the television camera is readily accessible. The image at point B in Figure 9 is in the form of an electronic signal referred to as the "composite video signal". This is transmitted from the camera via wires to the television monitor and/or a video tape-recording unit.

Analysis of composite video signal. The camera tube scans the output phosphor of the intensifier in a raster of sequential horizontal lines. The brightness of the image is represented by the voltage of the video signal from the camera. The position of a point in the image becomes a function of time due to the sequential scanning.

If the intensity variation along a horizontal line can be recorded while the square wave test pattern is being imaged, then the response of the system up to Point B (Figure 9) can be determined.

The composite video signal contains both the intensity information and synchronizing pulses which, by sequential scanning on the monitor, allow the image to be reproduced with spatial relationships preserved. In this experiment a single horizontal line is displayed on an oscilloscope so that intensity variation can be recorded. A special "line-select" device was designed and constructed to trigger the oscilloscope. This device is described in the Appendix. Figure 13 is an oscilloscope photograph of the electrical image of the square wave test pattern. The negative pulses at the left and right of the photo

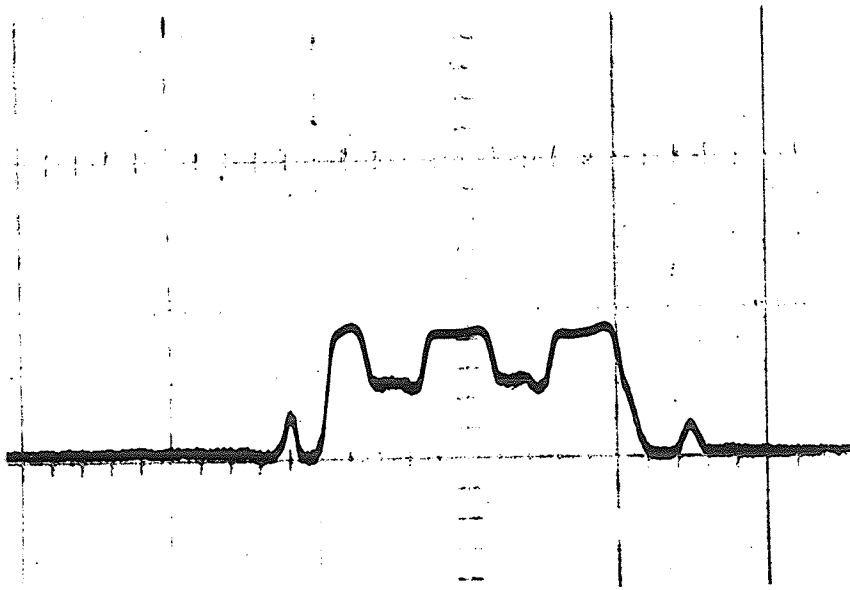


FIGURE 13  
OSCILLOGRAPH OF COMPOSITE VIDEO IMAGE  
OF SQUARE-WAVE PATTERN

are horizontal synchronizing pulses marking the beginning and end of the video line.

The intensity data was recorded in one of two ways. Either an oscillograph similar to Figure 13 was taken with a Nikon 35 mm. oscilloscope camera or a tracing was made on acetate directly from the oscilloscope screen. In either case the trace was transferred onto coordinate paper. The result is a graph of voltage (or image intensity) versus time on the oscilloscope sweep. The latter can easily be converted to correspond to position in the object plane.

An MTF obtained in this manner is plotted in Figure 14. Again, the MTF values calculated by the computer have been divided by those of the primary imaging process. All MTFs have been normalized at zero spatial frequency.

Interpretation of the results of MTF determinations will be attempted in the next chapter.

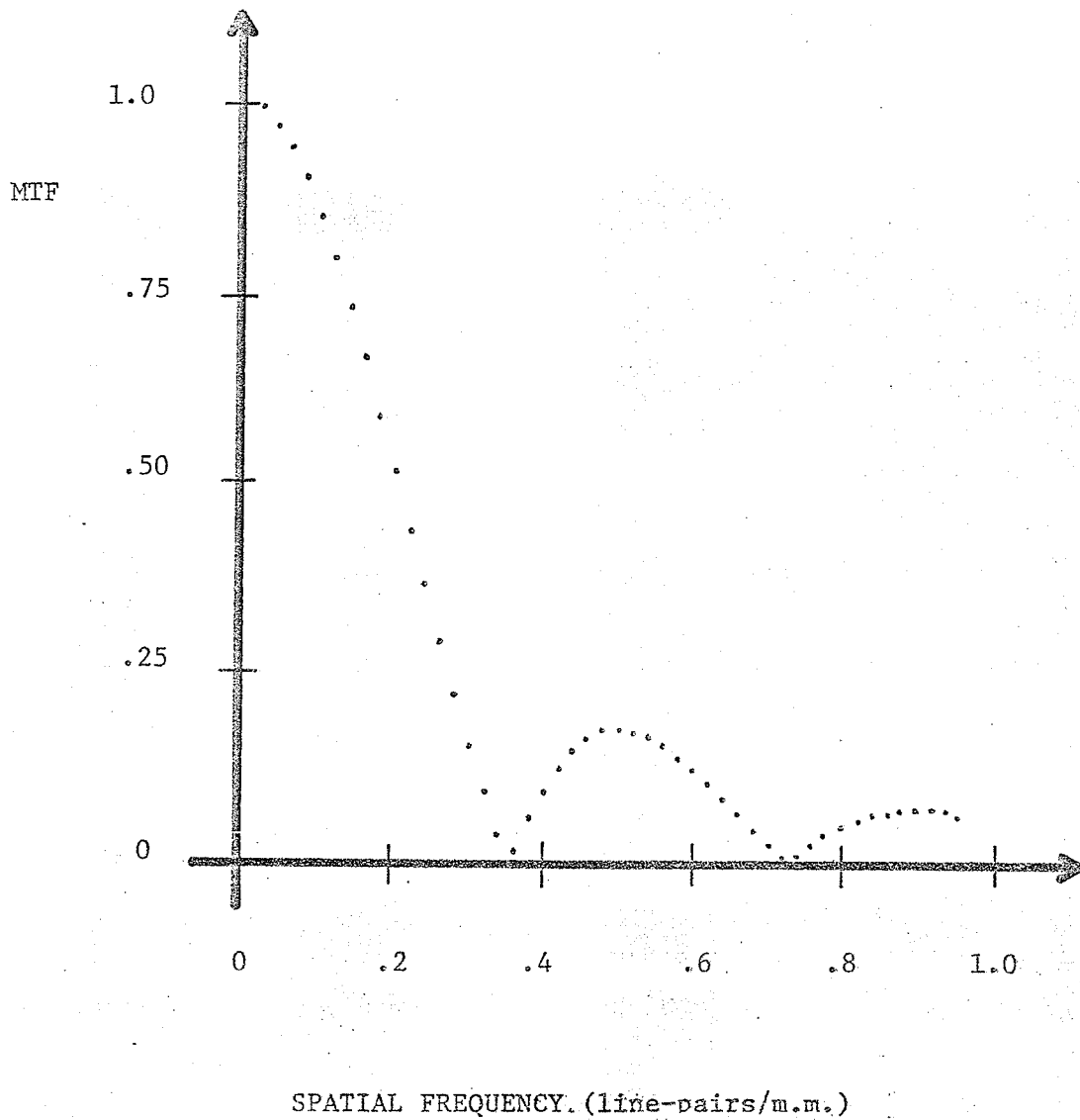


FIGURE 14  
MTF OF IMAGE INTENSIFIER  
AND TELEVISION CAMERA

## CHAPTER IV

### ASSESSMENT OF THE EXPERIMENTAL METHOD

In the preceding chapter modulation transfer functions were determined at three points in the fluoroscopic system of Figure 9. For convenience in comparison, the MTFs of Figures 8, 12 and 14 have been replotted in Figure 15.

#### MTF of primary imaging process

Curve A shows the MTF calculated from a radiographic exposure in the primary image plane. It is apparent that over the useful spatial frequency range of the IITS (0-1 lp./mm.), the response of the primary MTF does not fall appreciably, and that this stage, therefore, does not significantly lower the overall response. Only with larger focal spots and/or greater primary magnifications will the primary-stage effects become important. A good analysis of the effect of focal spot size and magnification on primary MTF is presented by Rao (24, 31).

#### MTF measured at the television monitor

No reports of overall MTF measurements for light amplifier systems, such as the Delcalix, could be found in the literature. Nevertheless it is still possible to compare our results with another measurement; that of the classical "resolution".

A standard copper foil resolution bar phantom manufactured by Picker X-Ray Corporation was used to compare the MTF with a subjective resolution measurement. Such measurements are the usual criteria for evaluation and adjustment of fluoroscopic systems.

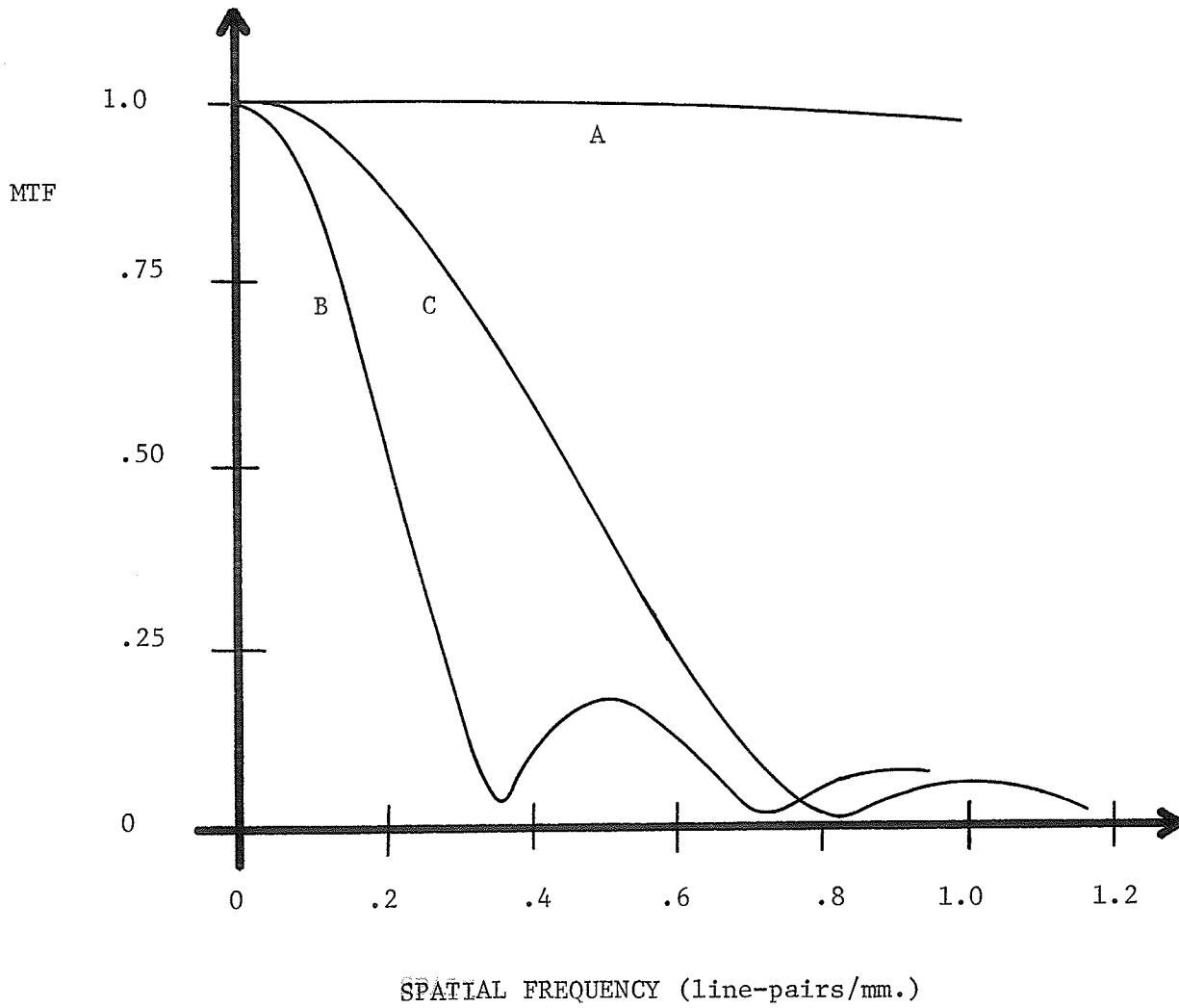


FIGURE 15  
MTFs OF COMPONENTS OF AN IMAGING SYSTEM  
(Measured at points A, B, and C of Figure 9)

A  $\frac{1}{2}$  inch thick aluminum plate was placed on the intensifier input phosphor. The bar phantom was positioned on the plate in the x-ray field. With the same geometry and x-ray settings employed in the experiment of Chapter III, two observers were asked to identify the highest frequency of bars in the pattern that could be seen. They were instructed to adjust the "brightness" and "contrast" controls of the monitor, if necessary, to obtain the highest resolution possible. They agreed that a pattern of 16 line pairs per inch (0.63 lp./mm.) could just be resolved while 20 line pairs per inch (0.8 lp./mm.) could not. Referring to Figure 15, Curve C, it is seen that the overall MTF between these frequencies falls from 18.5% to 1.5%. In their work on resolution measurements Bouwers (21) and Niklas (32) set the threshold modulation for visible resolution in fluoroscopy at 5%. Although there is no general agreement on the value of the threshold because of the complex nature of visual physiology and on the variation of contrast perception with image brightness, 5% falls within the range of generally accepted values. The MTF then agrees with the "resolution" within the uncertainty limits of the resolution measurement.

Influence of the television monitor -- contrast enhancement. As was indicated in the description of the experiment (Chapter III, page 33), the monitor was adjusted according to subjective criteria, by the operator. This is also the way in which it is adjusted during clinical operation.

The television monitor has a characteristic curve analagous to

that of a film. This curve is a composite of the characteristics of the electronic and electron-optical components of the monitor.

The "brightness" and "contrast" controls effectively determine the portion of the characteristic curve that is used.\* For a specific contrast in the video input signal to the monitor, the contrast on the monitor screen is determined by the shape of the characteristic curve at the point corresponding to the input. By changing the portion of the curve being used, an amplification of contrast or modulation is achieved.

Adjustment of the monitor controls can create a situation in which modulation in the monitor image is greater than the modulation in the input signal corresponding to that image. The modulation transfer function of the monitor is, therefore, adjustable and can be greater than unity at certain spatial frequencies. This gives rise to the phenomenon depicted in Figure 15 where the MTF measured at the monitor (Curve C) is actually greater at some frequencies than that measured after the preceding stage (Curve B).

It is possible to demonstrate the control of MTF by imaging the resolution phantom and adjusting the "brightness" and "contrast". The resolution point on the MTF can be lowered so that less than 0.5 lp./mm. can be seen or raised until .63 lp./mm. can be visualized. The bar pattern contained no lower frequencies than 0.5 lp./mm. so that further decrease in resolution could not be shown.

\*Zworykin's book on television theory (33) explains the relationship between the "contrast" and "brightness" controls.

Because of the large effect of monitor controls on MTF the statement of an MTF at the monitor has meaning only if the monitor operating conditions can be specified. Adjustment to produce the "best picture" will vary among operators and adjustment for best resolution is not necessarily the optimum setting of the monitor as lower spatial frequencies are then generally sacrificed. In any case the "contrast" and "brightness" settings should be quantified and specified allowing reproducibility of measurement.

Raster lines. When a photograph of the monitor is taken, the negative consists of an image of the raster lines and the spaces between. The microdensitometer scans the transmittance of both the lines and the spaces. The spaces are approximately uniformly illuminated on the monitor, and in the scan they will affect only the average value of the photometer readings, not the changes. Background subtraction is used to eliminate the effect of the spaces.

MTF of the composite video signal. Measurements of this type have been performed by other authors. Moseley (23) made measurements from an oscilloscope screen on the trace of the composite video signal with an entire frame of lines superimposed. As mentioned in Chapter II he actually measured the contrast transfer function rather than the MTF. His technique eliminated the need to perform Fourier analysis, but gave only an approximation to sine wave response. It is limited in the highest frequency that can be measured because test patterns above about 2 lp./mm. cannot easily be constructed.

Silverman (34) performed a similar experiment, except that he observed only a single horizontal line from the raster and used the oscilloscope trace qualitatively for instrument adjustment. He recorded the response as a "bar-spread" photographed from the oscilloscope screen. Since the Fourier analysis only changes the mode of presentation of the information displayed on the scope, nothing is lost by using only the spread function, except the ability to combine mathematically the results of image quality measurements of components in tandem. Silverman's approach is then useful for servicing evaluation but not for quantification of results.

Timmer (35) at Philips, Eindhoven, used a fine wire as a line absorber and produced effectively a negative line spread function. This function was recorded from several video lines and signal-averaged to produce a clean input to a Fourier transform program. This method has two possible advantages over the one described here. First, the Fourier spectrum of a square wave rapidly decreases with frequency whereas a line has a flat Fourier spectrum. The calculation of the MTF for a stage involves dividing the Fourier amplitude of the output of that stage by that of the input. If the input amplitude is very small (as it will be for a square wave at high frequencies) then any noise whatsoever in the output will cause the MTF to "blow-up". This problem only occurs when the frequency response of a component extends to high harmonics of the fundamental.

Timmer used a 100 micron wire as a test object. At 10 lp./mm.

the frequency response of the primary image of the wire had fallen to about 33%. Reference to Figure 8 indicates that this is no better than that of the square wave. In order to approach the response of a line source, the wire must be much finer than 100 microns. In any case, the response of the imaging systems evaluated here and by Timmers was sufficiently low that either test pattern was acceptable for MTF measurements.

### Conclusion

It has been found that satisfactory measurements of the MTF can be made using a square-wave test object of fairly low spatial frequency and analyzing the Fourier components of its image. A procedure for determining the modulation transfer function of components or processes whose outputs can be recorded on film has been described and measurement of the MTF at two such points in a modern fluoroscopic system has been carried out. The results of the overall MTF measurement were found to agree with the value of the subjective resolution of the system. This method can also be used for measurement of the MTF at the intensifier output phosphor in cases where this is accessible.

A method of measuring MTF from the composite video signal was also described. This method does not require microdensitometry or the production of sensitometric films. A device for displaying the composite video on an oscilloscope was designed and built and used to determine the MTF of part of a fluoroscopic system.

If immediate data on image quality are needed, the Fourier analysis can be omitted and the oscilloscopic trace of the image of a square wave can be used for adjustment of components. For mathematical combination of component responses the Fourier analysis must be done.

The MTF is a useful descriptor of the resolution characteristics of imaging systems. It can provide valuable data to enable evaluation and comparison of multicomponent systems. The evaluation of an overall MTF is a relatively time-consuming task, due to the necessity for photographic processing, mounting, scanning, etc.. In many cases observation of a single video line on the oscilloscope will provide sufficient qualitative information for maintenance procedures. It is felt that the objectivity of this technique provides a significant improvement over methods presently used by service personnel.

A program to measure the modulation transfer functions of a variety of intensifier fluoroscopic units in use in Manitoba is presently underway and a report is forthcoming.

APPENDIX

## APPENDIX

### LINE SELECTION AND IDENTIFICATION

#### Television scanning and synchronization

The image on the output phosphor of the intensifier is scanned by the pickup tube of the television camera and reproduced on the monitor as a raster of sequential horizontal lines. Scanning starts at the upper left corner of the image field and ends at the lower right corner. In the standard North American system there are 30 complete images or frames scanned per second. Each frame consists of 525 horizontal lines. Most of these contain video information, however some are lost in vertical retrace while the scanning beam travels from the lower right corner back to the upper left to begin the next frame.

To avoid flicker due to the 30 hertz frame rate, each frame is scanned in two interlaced fields of 262½ lines each. One field contains odd-numbered horizontal lines and the next, those that are even-numbered. The interlaced-field frequency of 60 hertz exceeds the critical fusion frequency of the eye so that the image appears without flicker.

The horizontal line rate is given by

$$30 \frac{\text{frames}}{\text{sec.}} \times \frac{525 \text{ lines}}{\text{frame}} = 15,750 \frac{\text{lines}}{\text{sec.}} .$$

Each horizontal line, therefore, lasts only 63.5 microseconds.

At the end of each horizontal line is a negative polarity horizontal synchronizing pulse responsible for keeping the camera and monitor scan lines in step with one another. These pulses can be seen in Figure 17 on Page 56. At the end of each field are wider vertical synchronizing pulses.

These are integrated by the camera and monitor vertical sweep circuits to produce timing pulses that keep the fields synchronized.

#### Display of a single line

The instantaneous voltage of the video signal represents the intensity at the corresponding point in the image. For an object whose radio opacity varies along one dimension only, the intensity distribution in its video image can be displayed on an oscilloscope, providing the object is oriented such that its opacity changes are perpendicular to the scan lines. It is necessary to separate the synchronizing information from the composite video and use it to trigger the oscilloscope. A device was designed and constructed for this purpose. A block diagram is shown in Figure 16.

First the negative synchronizing pulses were separated from the positive video intensity signal. An integrated-circuit sync separator (Motorola MC1345P) was used for this purpose. This also amplified the synchronizing pulses. Next the pulses were applied to an R-C low pass network which integrated the longer vertical pulses and thereby separated them from the horizontal pulses.

A Tektronix Type 555 Dual Beam dual time-base oscilloscope was used for display. The vertical synchronizing pulses were applied to the preamplifier of the upper trace of the oscilloscope. The upper sweep was set to run at a rate of 30 hertz. and was triggered by the vertical pulses.

The complex video signal from the television camera was applied

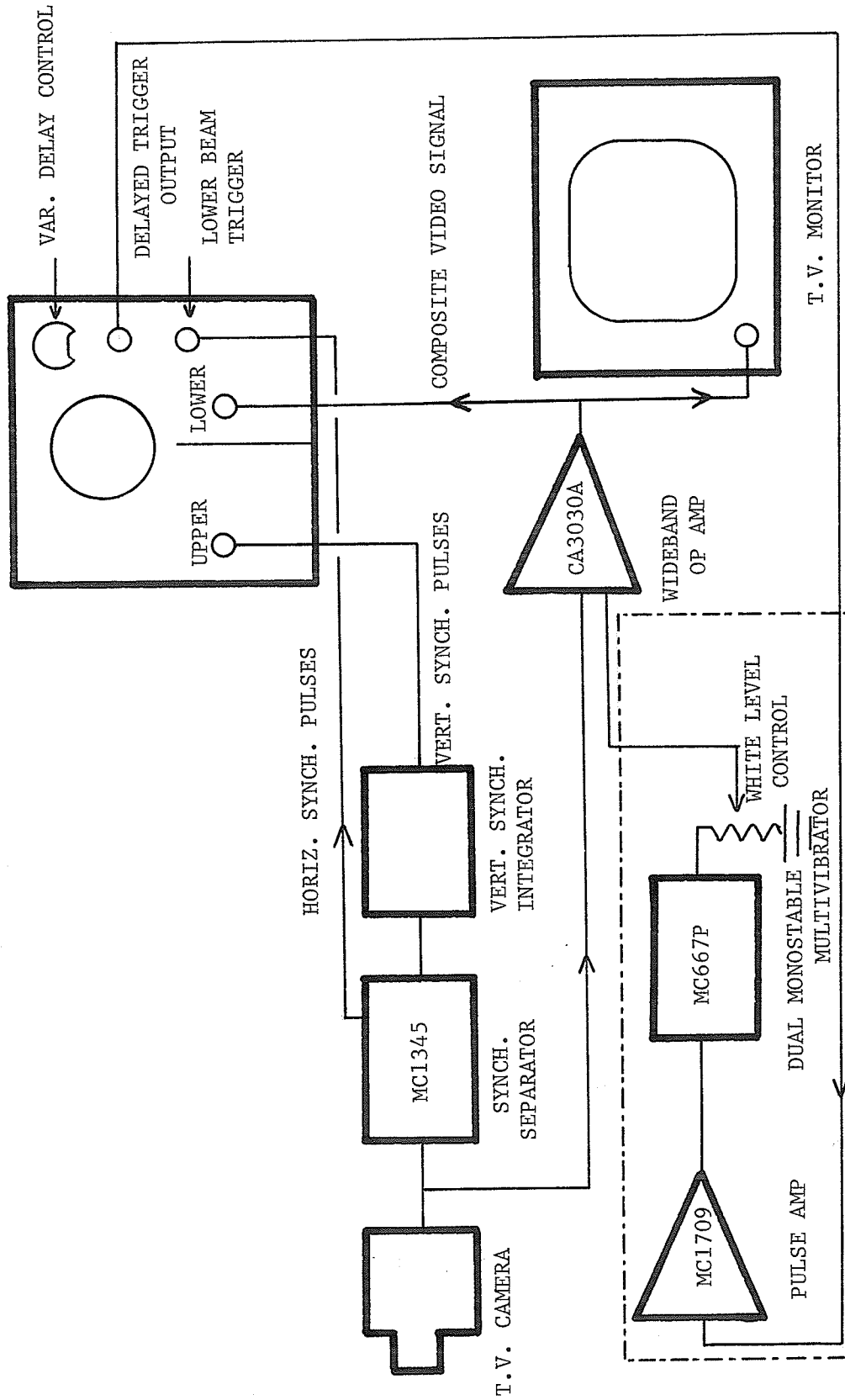


FIGURE 16  
LINE SELECTION AND IDENTIFICATION DEVICE

to the lower-trace preamplifier. The sweep was adjusted so that only one television line (63.5 microseconds) could be seen on the lower trace. With normal triggering of the sweep, consecutive lines in the frame would be superimposed as in the upper trace of Figure 17.

A particular video line is repeated every  $1/30$  second; i.e., once after each triggering of the upper trace of the oscilloscope. The Tektronix Type 555 is equipped with a "variable delayed-triggering" feature. This allowed the lower-beam sweep to be triggerable only after a pulse from the upper beam sweep. Each time the upper-beam sweep was triggered by the vertical pulses (30 times per second), a delay trigger pulse was transmitted to the lower-beam sweep. The time interval between the occurrence of the vertical frame pulse and the arrival of the delay trigger pulse at the lower-beam sweep was controlled by a variable delay.

Thus the lower beam was triggerable only once after each frame pulse and the point in each frame at which this happened could be adjusted. When triggerable, the lower beam was triggered by the horizontal synchronizing pulses from the sync separator.

In this way a video line lasting only 63.5 microseconds and occurring only 30 times per second could be displayed with good stability and the intensity distribution along it could be recorded. An oscillograph of a single triggered video line is shown in the lower trace of Figure 17.

In practice the lower-beam time-base was operated at 5 microseconds/cm. with sweep magnification of 5 times yielding a display of 1 microsecond/cm..

The bandpass of the oscilloscope electronics was 30 MHz.. The

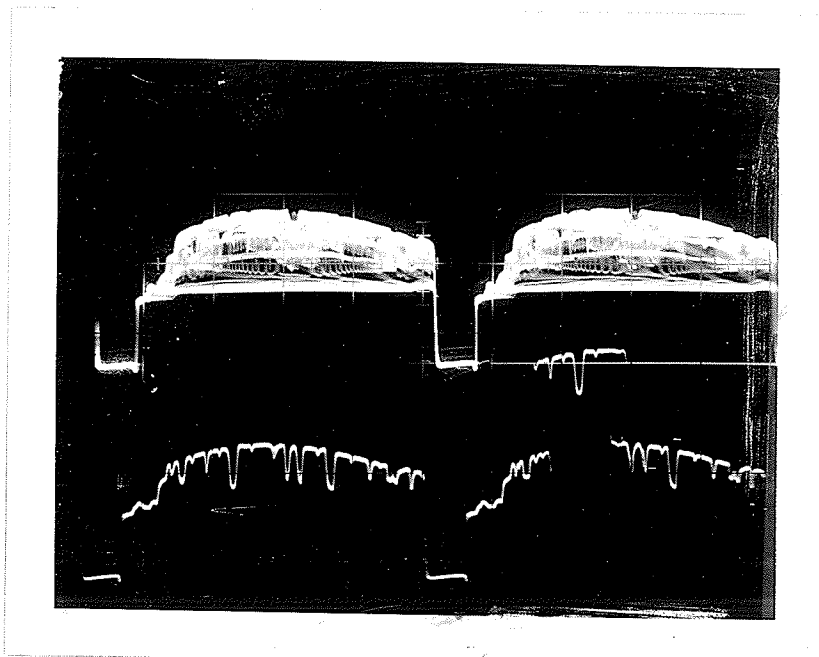


FIGURE 17

COMPOSITE VIDEO SIGNAL

(Upper) All lines in a frame are superimposed

(Lower) A single horizontal line is triggered

bandpass of x-ray television systems rarely exceeds 10 MHz. and in most cases is about one half that value. The oscilloscope was, therefore, considered a sufficiently sensitive measuring device for this experiment.

#### Line identification

As well as selecting particular raster lines for measurement, it was necessary to identify the line being viewed on the oscilloscope. A circuit was designed for this purpose. A schematic diagram of the line-selection and line-identification is given in Figure 18.

The delay trigger pulse from the oscilloscope was passed through an operational amplifier (Motorola MC1709) and applied to the trigger input of one half of an MC667P dual monostable multivibrator. The monostable was adjusted to remain "on" for 63.5 microseconds when fired. The output of the monostable was wired to the trigger input of the second half of the module so that when the first switched "off" the second switched "on". The "on" time of this monostable was adjustable between 0 and 63.5 microseconds. Each time a line was triggered on the oscilloscope, the second monostable switched "on" after a delay of one line period.

The output of the second monostable was coupled to the input of an RCA CA3030A wideband operational amplifier where it was added to the video signal. The output of the amplifier went to the television monitor. When the monostable was "on", a line segment of the line immediately following the one being viewed on the oscilloscope was shown brightened on the monitor. The length and brightness of the line segment was adjustable.

Electronic Components

C <sub>1</sub> - 1.0 mfd.	R <sub>6</sub> - 2200
C <sub>2</sub> - .1 mfd.	R <sub>7</sub> - 10 K
C <sub>3</sub> -10 pfd.	R <sub>8</sub> - 10 K
C <sub>4</sub> - .05 mfd.	R <sub>9</sub> - 2.2 K
C <sub>5</sub> - .101 mfd.	R <sub>10</sub> - 680
C <sub>6</sub> - .001 mfd.	R <sub>11</sub> - 680
C <sub>7</sub> - 5 pfd.	R <sub>12</sub> - 270
C <sub>8</sub> - 4700 pfd.	R <sub>13</sub> - 4.7 K
C <sub>9</sub> - 5 pfd.	R <sub>14</sub> - 100 K
C <sub>10</sub> - 150 pfd.	R <sub>15</sub> - 68 K
C <sub>11</sub> - 5 pfd.	R <sub>16</sub> - 1 K
C <sub>12</sub> - .0047 mfd.	R <sub>17</sub> - 47 K
C <sub>13</sub> - .003 mfd.	R <sub>18</sub> - 1.5 K
R <sub>1</sub> -	R <sub>19</sub> - 1.5 K
R <sub>2</sub> - 2.2 K	R <sub>20</sub> - 39 K
R <sub>3</sub> - 330 K	R <sub>21</sub> - 1.5 K
R <sub>4</sub> - 100 K	R <sub>22</sub> - 4.7 K
R <sub>5</sub> -	R <sub>23</sub> - 1.5 K

External Connections

- P<sub>1</sub> - video signal from camera
- P<sub>2</sub> - horizontal sync pulses to lower-beam trigger
- P<sub>3</sub> - vertical sync pulses to upper beam-trigger
- P<sub>4</sub> - chassis ground
- P<sub>5</sub> - video signal to lower-beam preamplifier
- P<sub>6</sub> - video and line-identification pulse to monitor
- P<sub>7</sub> - delay-trigger pulse from oscilloscope

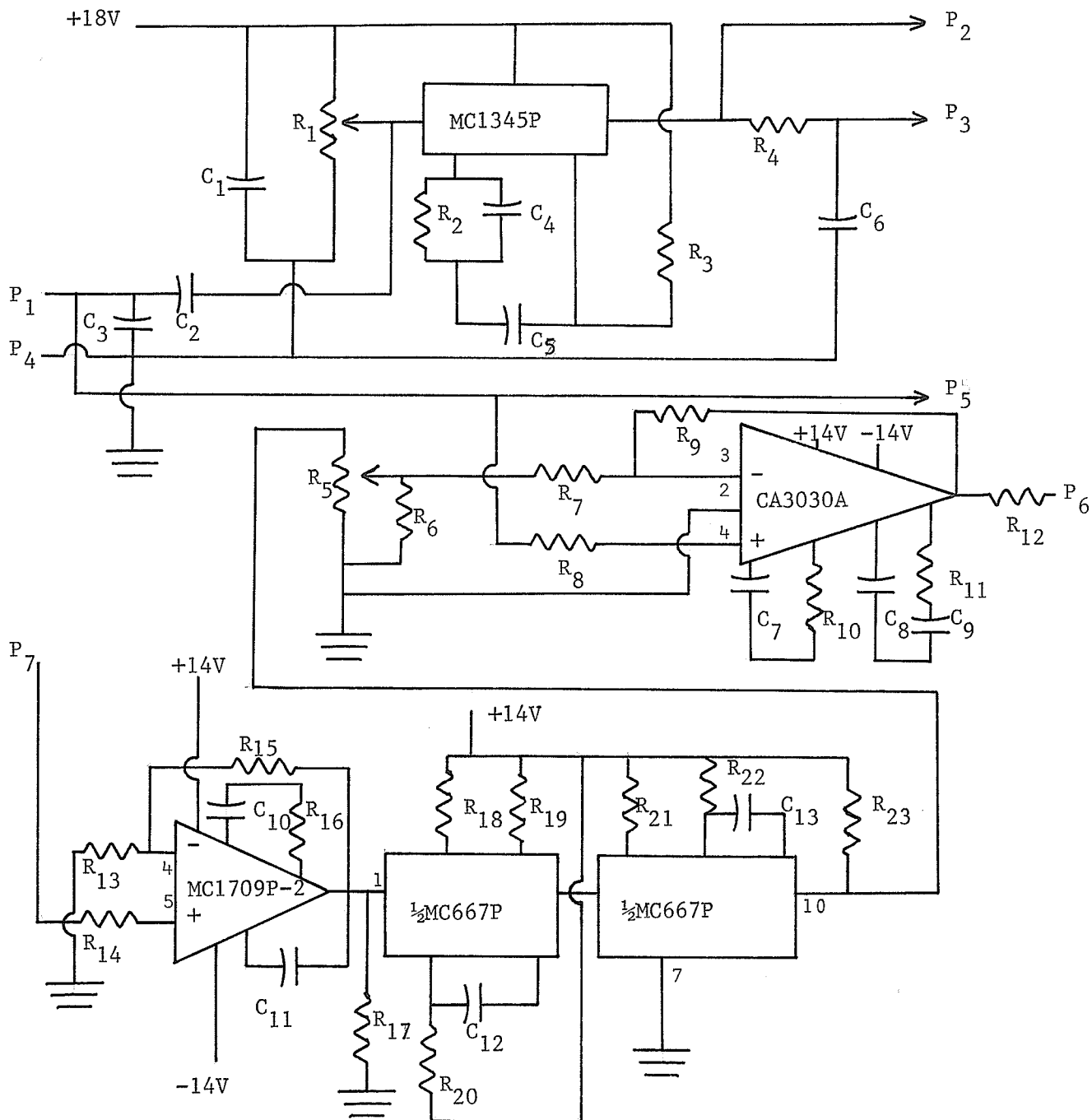


FIGURE 18  
 SCHEMATIC DIAGRAM OF LINE SELECTION  
 AND IDENTIFICATION CIRCUITS

This system allowed easy identification and measurement of any line in the television raster.

LIST OF REFERENCES

LIST OF REFERENCES

1. R. Jones and O. Lodge, *The Lancet*, 1, 476, (1896).
2. J. MacIntyre, *The Lancet*, 4, 1303, (1896).
3. W. E. Chamberlain, *Radiology* 38, 383, (1942).
4. J. W. Coltman, *Radiology* 51, 359, (1948).
5. H. E. Johns and J. R. Cunningham, *The Physics of Radiology*, (Charles C. Thomas, Springfield, 3d. ed., 1969) p. 588-591.
6. W. S. Properzio and E. Dale Trout, *Radiology* 91, 439, (1968).
7. E. W. H. Selwyn, *The Photographic Journal* 88B, 6, (1948).
8. F. H. Perrin, *J. Soc. Motion Picture and Television Engrs.* 69, 151, (1960).
9. J. W. Coltman, *Radiology* 51, 359, (1948).
10. G. M. Ardran and H. E. Crooks, *The Modulation Transfer Function: Practical Considerations in Medical Radiology. In Diagnostic Radiologic Instrumentation -- Modulation Transfer Function*. (Charles C. Thomas, Springfield, 1965), p. 142.
11. B. J. O'Loughlin, *Evaluating Image Quality. In Diagnostic Radiologic Instrumentation -- Modulation Transfer Function*. (Charles C. Thomas, Springfield, 1965), p.30.
12. K. Rossmann, *Am. J. Roentgenol.* 97, 772, (1966).
13. P. Marhoff and O. Schott, *Relationship between Dose Rate, Characteristics of the Image-Intensifier Television Chain, and Image Quality. In Diagnostic Radiologic Instrumentation -- Modulation Transfer Function*. (Charles C. Thomas, Springfield, 1965) p.25
14. A. W. Templeton, S. J. Dwyer, C. Jansen, L. Garrotto, J. E. Rathke, and J. H. Tolan, *Radiology* 91, 725, (1968).
15. G. A. Hay, *Radiology* 83, 86, (1964).
16. R. E. Sturm and R. H. Morgan, *Am. J. Roentgenol.* 62, 617, (1949).

17. W. Kuhl, Information Transfer with Image Intensifier Systems. In Diagnostic Radiologic Instrumentation -- Modulation Transfer Function. (Charles C. Thomas, Springfield, 1965), p.222.
18. R. Wipfelder, H. P. Pendergrass, and E. W. Webster, Radiology 88, 355, (1967).
19. K. Rossmann, Am. J. Roentgenol. 90, 178, (1963).
20. K. Rossmann, Radiology, 93, 257, (1969).
21. A. Bouwers. The Practical Value of Contrast Transfer in Radiology. In Diagnostic Radiologic Instrumentation -- Modulation Transfer Function. (Charles C. Thomas, Springfield, 1965) p. 3.
22. R. D. Moseley, Jr., T. Holm, and I. H. Low, Am. J. Roentgenol. 92 418, (1964).
23. R. D. Moseley, Jr., T. Holm and J. R. Williams. Composite Modulation Transfer Functions of Image Intensifier Television Systems. In Diagnostic Radiologic Instrumentation -- Modulation Transfer Function. (Charles C. Thomas, Springfield, 1965), p. 180.
24. G. U. V. Rao. The Modulation Transfer Function in Radiology and Nuclear Medicine. 14th Annual Meeting of AAPM, Philadelphia, June 26-29, 1972.
25. G. Lubberts and K. Rossmann, Phys. Med. Biol., 12, 65, 1967
26. Radiography in Modern Industry, 2d.ed. (Eastman Kodak Company, X-Ray Division, Rochester, 1957).
27. W. M. Gentleman and G. Sande, 1966 Fall Joint Computer Conference, AFIPS Proc. 29, 563, 1966.
28. Control Data (La Jolla Division), Programming Specification Number 84897200, 1968.
29. J. W. Cooley and J. W. Tukey, J. Math. Comp., 19, 297, (1965).
30. R. L. Lamberts and C. M. Straub, Phot. Sc. & Eng., 9, 335, (1965).

31. G. U. V. Rao and L. M. Bates, *Phys. Med. Biol.*, 14, 93, (1968).
32. W. F. Niklas. Noise Considerations in X-Ray Image Tube Design. In Diagnostic Radiologic Instrumentation -- Modulation Transfer Function. (Charles C. Thomas, Springfield, 1965), p. 312.
33. V. K. Zworykin and G. A. Morton, TELEVISION, (John Wiley, New York, 1940) p.172-175.
34. N. R. Silverman and G. Hylander, *Am. J. Roentgenol.* 110, 172, (1970).
35. F. Timmers, Evaluation of X-Ray Imaging Systems in Terms of Transfer Function. IEE/IERE meeting on X-ray Image Intensifier Systems, London June 14, 1973.
36. K. Rossman, A.G. Haus, and K. Doi, *Phys. Med. Biol.*, 17, 648, (1972).
37. C.E. Metz, K.A. Strubler, and K. Rossman, *Phys. Med. Biol.*, 17, 638, (1972).

## CORRESPONDENCE BETWEEN A SINUSOIDAL OBJECT AND ITS IMAGE

If an imaging system is ideal the illumination at any point of an image will correspond to and arise from its counterpart in the object plane. Thus the image will be a faithful representation of the object differing only in its magnification.

If the imaging system is not ideal then light which, in the ideal system, would be imaged at a point, will be distributed over an area surrounding this point.

Let  $z$  be a distance in the negative  $x$  direction from the ideal imaging point,  $x$ , and let the imaging system cause a point ideally imaged at  $x$  to give an intensity distribution of  $\phi(z)$ .

Let us consider an object varying only in the  $x$  direction in a sinusoidal fashion. Since the object is constant at right angles to the  $x$  direction, variations in intensity due to the imaging system need only be considered in the  $x$  direction.

If this object is imaged by an ideal system the intensity of the image may be represented by

$I_0 (1 + \alpha \sin mx)$  where  $\frac{1}{m}$  is the lateral magnification of the system.

In the real system however the intensity at a point will be

$$I_x = \int_{-\infty}^{+\infty} I_0 \{1 + \alpha \sin (mx + z)\} \phi(z) dz$$

due to the super position of intensity distributions from neighbouring points.

$$I_x = I_0 \int_{-\infty}^{+\infty} \phi(z) dz + I_0 \alpha \sin mx \int_{-\infty}^{+\infty} \cos mz \phi(z) dz + I_0 \alpha \cos mx \int_{-\infty}^{+\infty} \sin mz \phi(z) dz$$

If the frequency of the sinusoidal variation is high or if  $m$  is high the latter two terms will approach zero, thus the intensity becomes uniform and equal to  $I_0$ .

$$\text{i.e. } \int_{-\infty}^{\infty} \phi(z) dz = 1$$

Thus the expression for  $I_x$  may be written in the form:

$$I_x = I_0 \{ 1 + \alpha P \sin (mx + w) \}$$

It can be seen that this is a sinusoidal wave form similar to the ideal image except for a phase and amplitude change.